NUREG-0062
NRC-2

TWO-PHASE PRESSURE DROP ACROSS RESTRICTIONS AND OTHER ABRUPT AREA CHANGES

B. Harshe
A. Hussain
J. Weisman

Manuscript Submitted to NRC: December 1975
Date Published: April 1976

Prepared for U. S. Nuclear Regulatory Commission under Contract No. AT (49-24)-0179

Department of Chemical and Nuclear Engineering
University of Cincinnati
Cincinnati, Ohio 45221

Abstract

As part of continuing study of steady state and transient two-phase pressure drop across abrupt area changes, steady state pressure losses across restrictions of varying geometries were determined using Freon-and Freon vapor. The results obtained are consistent with one-dimensional momentum balance theory which indicates that the prediction equation to be used depends upon whether or not the vena contracta lies within the insert. Each of these equations requires a knowledge of the void fraction at the inlet, outlet and vena contracta. It was found that, for very short inserts (Ratio of restriction length, L, to diameter, D, less than 0.5) pressure drops were best predicted assuming slip flow at all locations while long inserts (L/D >2.5) required the assumption of slip flow at inlet and outlet and that the void fraction at the vena contracta was at or near the homogeneous value. For intermediate length inserts, partial mixing at the vena contracta must be assumed. A chart allowing the prediction of the degree of mixing at the vena contracta in intermediate length inserts is presented.

The mass flow rates used in these experiments were all at or above 4×10^5 lbs/hr ft^2 in the small size pipe or restriction. Caution should therefore be used in extrapolating these results to very low flow rates.

Contents

ACKNOWLEDGEMENT

The authors wish to acknowledge the financial support of the Division of Reactor Safety Research of the Nuclear Regulatory Commission. The assistance of Reactor Safety Research personnel is appreciated. In particular, the help and criticism of Mr. Aleck Serkiz is gratefully acknowledged.

1.0 Introduction

1.1 Background

The work presented in this report is part of a continuing study of steady state and transient two-phase pressure drops across abrupt area changes. The results of studies of pressure drop across well separated abrupt expansions and contractions during steady state were presented in report COO-2152-15. Data obtained across well separated expansions and contractions during oscillatory flow have been presented in report COO-2152-18.[1]

As a result of the previous studies, two-phase pressure drop across well separated area changes is believed to be fairly well understood for small scale systems. However, the previous data in the literature indicated that when an abrupt expansion and contraction were in close proximity (i.e-at a flow restriction) then behavior was somewhat different than for well separated area changes. However, the results reported in the literature were not entirely consistent. Further, the data available were insufficient to determine when the behavior changed from that of a well separated area change to that of a thin (short L/D) restriction.

1.2 Objectives of Present Tests

The purpose of this reported research was to provide a coherent view of two-phase pressure drop across area changes and restrictions during steady state flow.

The specific objectives of the present test program were to:

a) Determine the limits for the application of the previously established one-dimensional momentum balance equations as the abrupt expansion and contraction are moved together.

b) Determine an appropriate model for description of the two-phase pressure drop behavior of short restrictions where the abrupt expansion and contraction were in very close proximity.

c) Determine an appropriate model for use in describing the transition from a well separated expansion-contraction behavior to that applicable when the expansion and contraction are in close proximity (short restrictions).

2.0 Results of Previous U.C. Test and Analysis Program

2.1 General Analysis Procedures

The previous analysis of the behavior of abrupt area changes was made with the assumption that one-dimensional momentum theory is justified. For this to be the case, the momentum balance must be made across planes which are sufficiently distant from the area change so that a one dimensional flow pattern may be assumed. The analysis has also assumed that the liquid and vapor velocities may be represented by single values at the planes across which the momentum balance is written. Further, it has been assumed that the pressure is essentially uniform across the pipe at these locations.

With these general assumptions, the equations describing the pressure drop across abrupt area changes can be written in terms of the total mass flow, quality and void fraction. If the assumptions may be considered as reasonable, the major difficulty remaining is that of determining the appropriate relationship between quality and void at the various locations appearing in the momentum balance.

2.2 Abrupt Expansions

An abrupt expansion, well separated from other area changes, is shown schematically in Fig. 1a. The momentum balance is taken across planes 1 and 2. In single phase flow, the inference is made that the upstream pressure, acts on the pipe wall at position "0". By use of this assumption, together with those delineated in the previous section, Lottes[3] reports that Romie obtained

$$\Delta p_E = \frac{G_T^2 \sigma^2}{\rho_l g_c}\left\{\left[\frac{\rho_l}{\rho_g} x^2\left(\frac{1}{\alpha_1 \sigma} - \frac{1}{\alpha_2}\right)\right] + \left[(1-x)^2\left(\frac{1}{\sigma(1-\alpha_1)} - \frac{1}{(1-\alpha_2)}\right)\right]\right\} \quad (1)$$

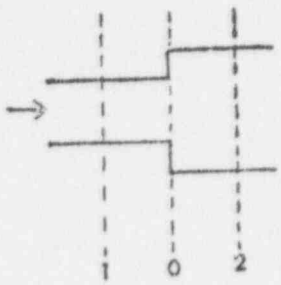

Fig. 1a Abrupt Expansion Schematic

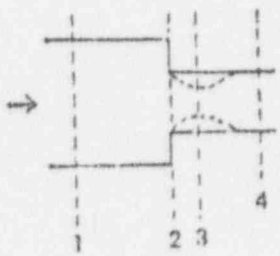

Fig. 1b Abrupt Contraction Schematic

where Δp_c = pressure rise between locations 1 and 2 assuming pipe friction is negligible

$\rho_g \rho_l$ = gas and liquid densities, respectively

G_T = total mass velocity based on area of smaller pipe (lbs/hr ft^2

x = quality (lb vapor/lb total fluid flowing)

σ = area ratio

α_1 α_2 = void fraction at locations 1 and 2 (see Fig 1)

Janssen[2] made a similar analysis and arrived at the same conclusion.

Previous studies at the University of Cincinnati[1] carefully examined the experimental steam-water data of Mendler,[4] Ferrell and McGee[5], Janssen and Kervinen[6] and Fitzsimmons[7]. When it was assumed that the flow was homogenous upstream and downstream of the expansion, the predicted pressure drops were higher than those observed for most cases (see Fig. 2) When slip, flow was assumed, reasonable agreement between prediction and observations were obtained (see Fig. 3). The values of α_1 and α_2 were estimated by use of Hughmark's[8] relationship between x and α_1. This correlation was chosen since it includes a velocity effect which leads to slip ratios approaching one at high fluid velocities. This is in accord with the visual observation that the flow tends toward homogeneous flow as velocity is increased. It also agrees with the observation that pressure drops predicted[9] by the homogeneous model approach those observed as the velocity is increased.

Husain, Choe, and Weisman[9] conducted a statistical analysis of the available expansion data. Following Dukler et al[10], they defined the average fractional deviation, $\bar{d}$, as

$$\bar{d} = \left(\sum_{i=1}^{n} d_i\right)/n \qquad (2)$$

where $d_i = (P_i - M_i)/M_i$

P_i = predicted value for i_{th} data points

M_i = measured value for i_{th} data point

n = number of data points

An estimate, s(d), of the standard deviation of d is then given by

$$s(d) = \sqrt{\frac{\Sigma d_i^2}{n} - \bar{d}^2} \qquad (3)$$

As shown in Table 1, Husain et al divided the available data into mass velocity ranges and determined $\bar{d}$ and s(d) for each range. It is clear that as the mass velocity, G, approaches 2×10^6 lbs/hr ft^2 (the value at which Husain et al. conclude the transition to homogeneous flow to occur) the homogeneous model predictions approach observations.

Statistical Comparison of Abrupt Expansion Data

	Homogeneous Model		Slip Flow	
	$\bar{d}$	s(d)	$\bar{d}$	s(d)
G* $\leq .5 \times 10^6$	0.60	.94	-0.02	.64
G $\leq 1 \times 10^6$	0.49	.82	-0.03	.54
G $\geq 1 \times 10^6$	0.05	.11	-0.08	.09
G $\geq 2 \times 10^6$	0.10	.06	-0.00	.08
all G	0.42	.77	-0.04	.49

*G based on mass velocity in larger pipe in above table.

Although $\bar{d}$ appears to increase slightly for G $\geq 2 \times 10^6$, Husain et al. concluded that the change was more apparent than real. Because of the small number of points with G $\geq 2 \times 10^6$, the difference in $\bar{d}$ is within the variability to be expected if the true universe means were the same in the 2 highest velocity ranges.

Fig. 2 Comparison of Pressure Rise Measured Across an Expansion With Pressure Rise Predicted by Using All Homogeneous Model.

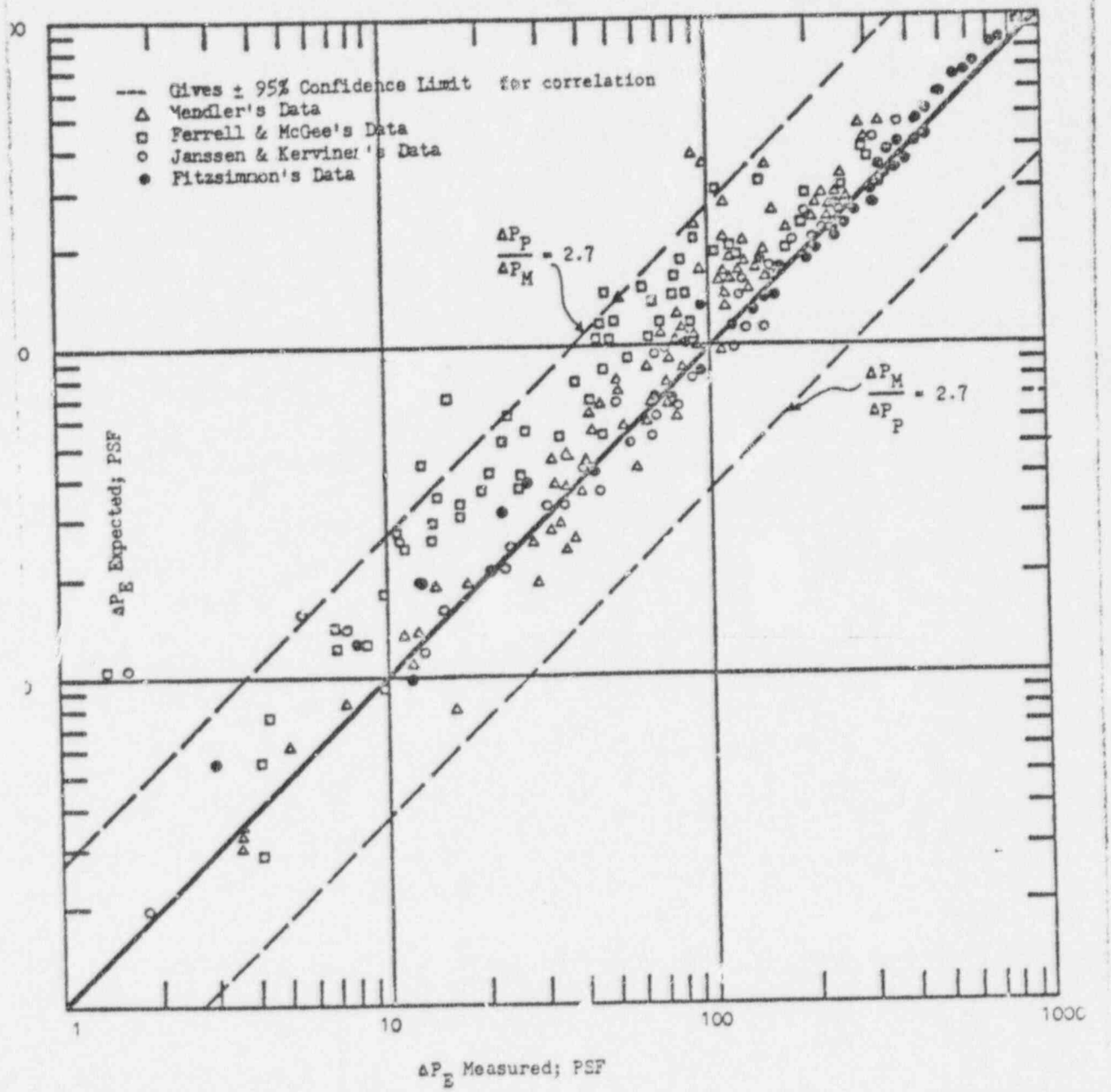

Fig. 3 Comparison of Pressure Rise Measured Across an Expansion With Pressure Rise Predicted by Using All Slip Model.

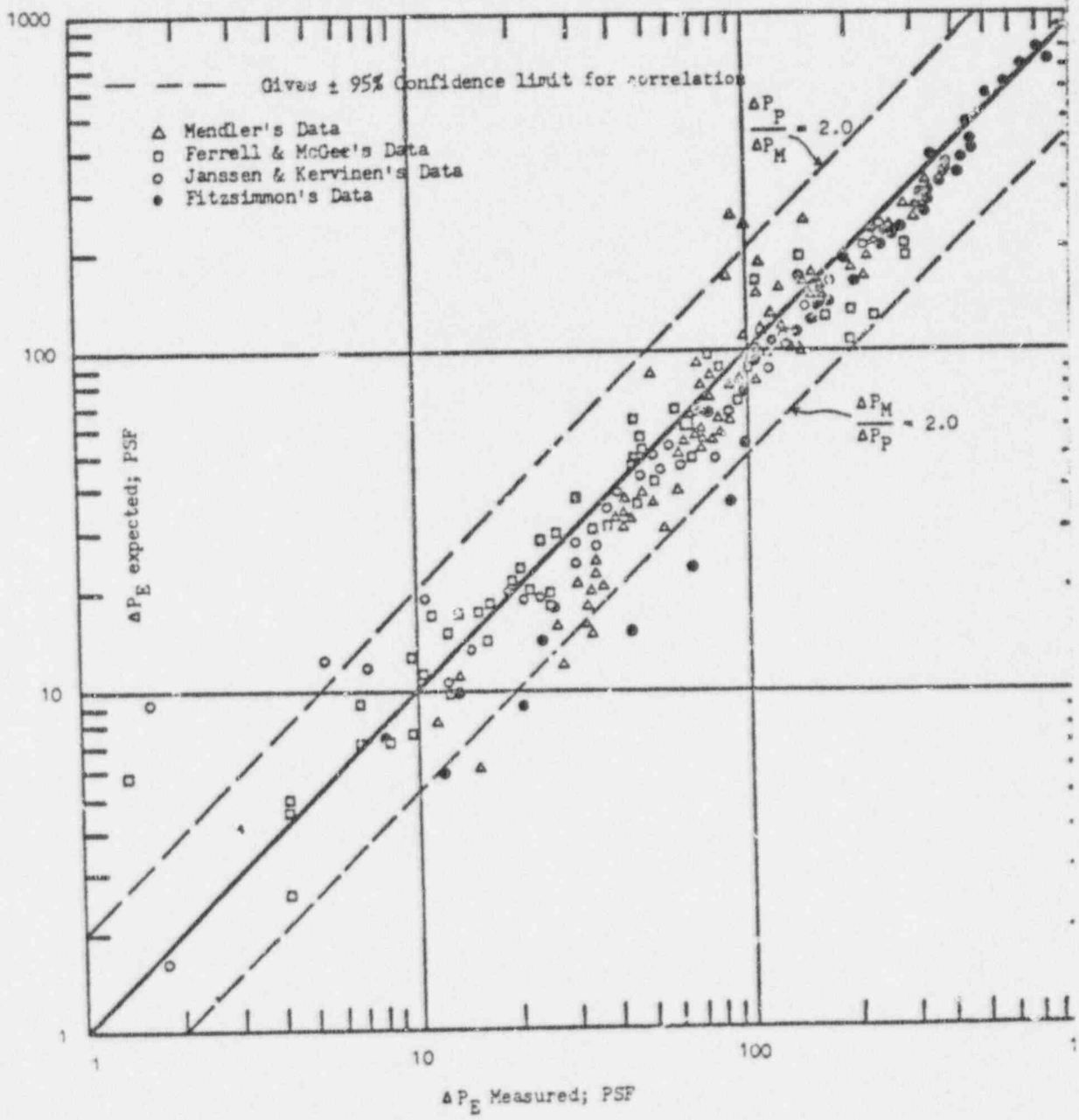

2.3 Abrupt Contractions

Janssen[2] applied a one-dimensional force momentum flux balance to two-phase flow across an abrupt contraction well separated from any other area change (see Fig. 1b). In addition to those assumptions indicated previously, Janssen assumed, just as generally done for single phase flow, that pressure P_3 (Fig. 1b) acts over the full area of the small pipe and that there are no frictional losses between sections 1 and 3. Under conditions where the pressure loss is small and x may be taken as a constant he obtained for ΔP_c, the pressure drop across the contraction, that

$$\Delta P_c = \frac{G_1^2}{2g_c \rho_1} \left[\frac{1}{\sigma^2} \left(\frac{\rho_1}{\rho_g} x^2 \bar{\alpha}_1 \left(\frac{1}{C^2 \alpha_3^2} - \frac{1}{\alpha_4^2} \right) + (1-x)^2 (1-\bar{\alpha}_1) \right. \right.$$

$$\left(\frac{1}{C^2(1-\alpha_3)^2} - \frac{1}{(1-\alpha_4)^2} \right) \Big) - \frac{2}{\sigma^2} \frac{\rho_1}{\rho_g} x^2 \left(\frac{1}{C\alpha_3} - \frac{1}{\alpha_4} \right) + (1-x)^2 \left(\frac{1}{C(1-\alpha_3)} - \frac{1}{(1-\alpha_4)} \right)$$

$$\left. + \frac{\rho_1}{\rho_g} x^2 \bar{\alpha}_2 \left(\frac{1}{\sigma^2 \alpha_4^2} - \frac{1}{\alpha_1^2} \right) + (1-x)^2 (1-\bar{\alpha}_2) \left\{ \frac{1}{\sigma^2(1-\alpha_4)^2} - \frac{1}{(1-\alpha_1)^2} \right\} \right] \qquad (4)$$

where G_1 = total mass velocity at Section 1 (Fig. 1b) lbs/hr ft^2

C = vena contracta area ratio

σ = channel area ratio (area small pipe/area large pipe)

x = mixture quality

$\alpha_1 \alpha_2 \alpha_3 \alpha_4$ = void fraction at sections 1,2,3 and 4, respectively

$\bar{\alpha}_1$ $(\alpha_3 + \alpha_3)/2$

$\bar{\alpha}_2$ $(\alpha_1 + \alpha_4)/2$

On the basis of his own steam-water data, Janssen[2] suggested that α_1, α_2 and α_4 be estimated by assuming slip flow at these locations. However, he suggested that α_3, the void fraction at the vena contracta,

be obtained by assuming homogeneous flow at this location. This agreed with Janssens' observation of strong mixing act.. at the vena contracta.

In the previous University of Cincinnati work, two-phase pressure drops across abrupt contractions were experimentally measured using Freon 113 as the working fluid. Contractions having area ratios (σ) of 0.25 and 0.56 were examined. The test section with $\sigma = 0.56$ was transparent and hence allowed visual observation. These observations also indicated strong mixing at the vena contracta.

A comparison was made of the University of Cincinnati Freon data and the steam-water data of Janssen[2] Geiger[11] and Fitzsimmons[7] with predictions obtained from Equation (4) using σ based on single phase data and various means for estimating void fractions. It was finally concluded that α_1, α_2 and α_4 should be estimated assuming slip flow at these locations. Again Hughmarks' correlation[8] was used to obtain the relationship between α and x. The value of α_3 (α at the vena contracta) was obtained from

$$\begin{aligned} \alpha_3 &= \alpha_{homogeneous}, && \text{for } \alpha \leq 0.5 \\ \alpha_3 &= \alpha_{slip} + A(\alpha_{homogeneous} - \alpha_{slip}), && \text{for } \alpha \geq 0.5 \end{aligned} \tag{5}$$

where $A = 1.5 - \alpha_4$

α_{slip} = value of α which be computed for vena contracta size pipe in absence of contraction, from correlation of Hughmark

$\alpha_{homogeneous}$ = void fraction based on slip ratio of 1.0

Fig. 4 shows the comparison of this model with the available experimental data.

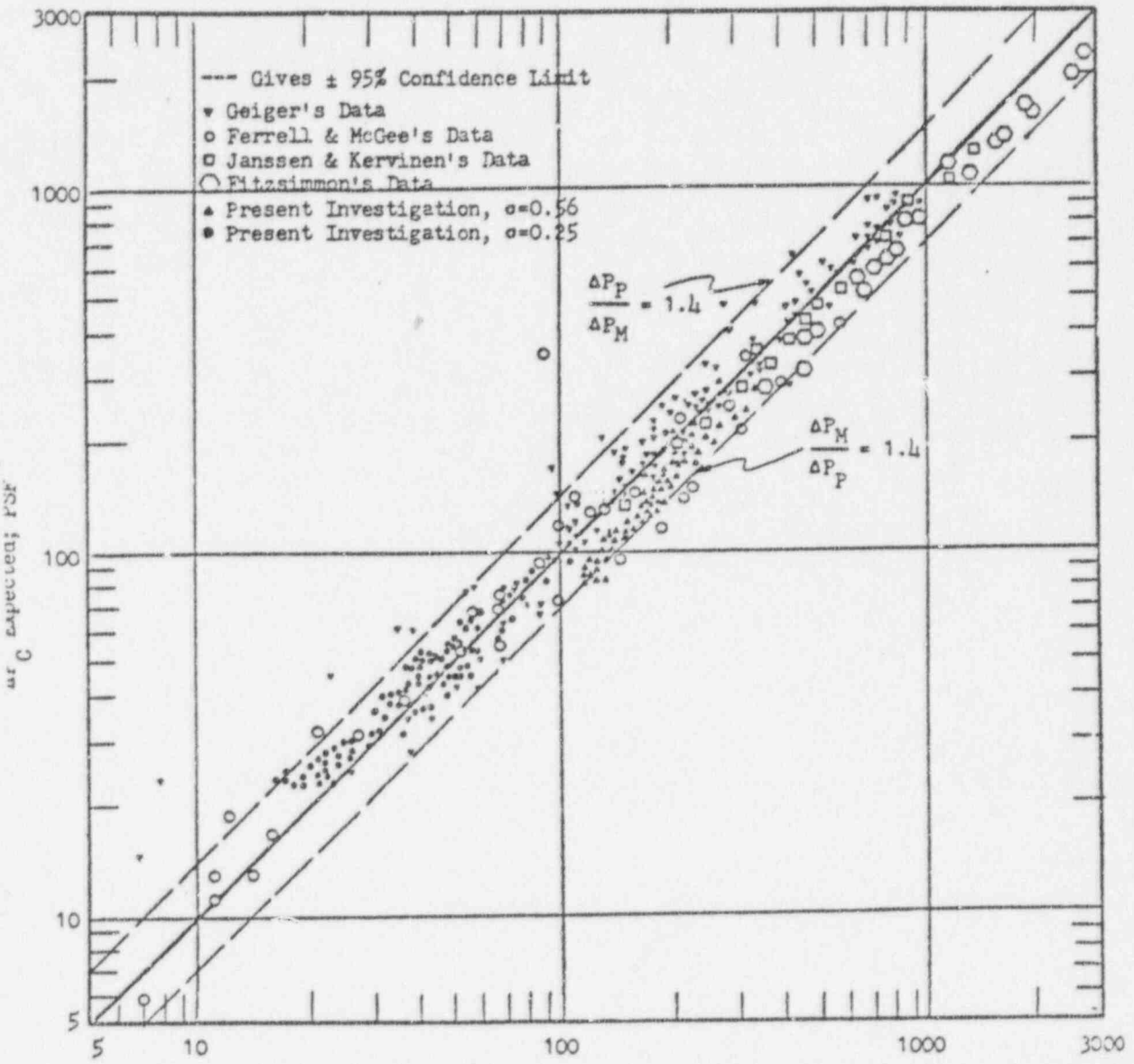

Fig. 4 Comparison of Pressure Drop Predicted by Eq. (4) and (5) with the Measured Pressure Drop Across an Abrupt Contraction.

Geiger[12] noted that his contraction pressure drop data could be reasonably correlated by assuming homogeneous flow-everywhere. It is seen in Fig. 5 that this approach provides nearly as good a correlation as that shown in Fig. 4. However, this procedure can only be regarded as a convenient approximation since it requires use with the Freon data of void fractions at locations 1 and 4 which were appreciably higher than those actually observed.

2.4 Well Separated Expansion - Contraction Combinations

The total pressure drop ΔP_L, across an expansion and contraction (not including pipe friction) which are separated by an appreciable distance should be obtained by simple summation of the pressure changes. Thus:

$$\Delta P_L = \Delta P_c - \Delta P_e \tag{6}$$

where ΔP_c and ΔP_e are obtained from Equations (1) and (5) respectively using the previously suggested methods for evaluation of void fraction. The summation yields

$$\Delta P_L = \frac{G^2}{2\rho_1 g_c}\left[\frac{1}{\sigma^2}\left(\frac{\rho_1}{\rho_g}x^2\bar{\alpha}_1\left(\frac{1}{C^2\alpha_3^2}-\frac{1}{\alpha_4^2}\right)+(1-x)^2(1-\bar{\alpha}_1)\right.\right.$$
$$\left.\left(\frac{1}{C^2(1-\alpha_3)^2}+\frac{1}{(1-\alpha_4)^2}\right)\right)-\frac{2}{\sigma^2}\left(\frac{\rho_1}{\rho_g}x^2\left(\frac{1}{C\alpha_3}-\frac{1}{\alpha_4}+\frac{\sigma}{\alpha_3}-\frac{\sigma^2}{\alpha_6}\right)\right.$$
$$\left.+(1-x)^2\left(\frac{1}{C(1-\alpha_3)}-\frac{1}{(1-\alpha_4)}+\frac{\sigma}{(1-\alpha_5)}-\frac{\sigma^2}{(1-\alpha_6)}\right)\right)+\frac{\rho_1}{\rho_g}x^2\bar{\alpha}_2$$
$$\left.\left(\frac{1}{\sigma^2\alpha_4}-\frac{1}{\alpha_1^2}\right)+(1-x)^2(1-\bar{\alpha}_2)\left(\frac{1}{\sigma^2(1-\alpha_4)^2}-\frac{1}{(1-\alpha_1)^2}\right)\right] \tag{7}$$

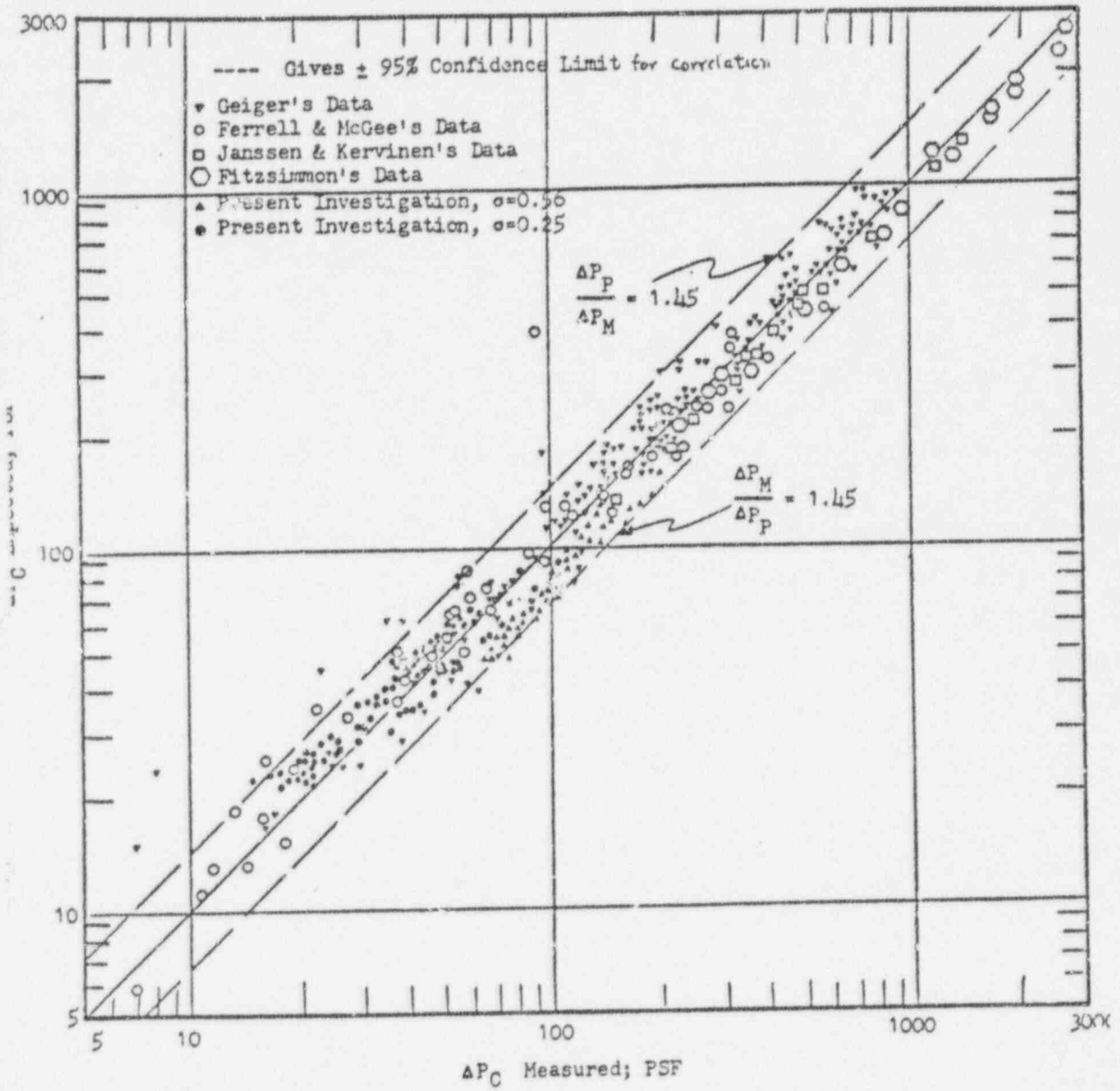

Fig. 5 Comparison of Pressure Drop Predicted by Homogeneous Model with the Measured Pressure Drop Across an Abrupt Contraction.

where G = total mass velocity in large size pipe, lb/hr ft^2

C = vena contracta area ratio

α_i = void fraction at i_{th} section

$\bar{\alpha}_i = (\alpha_3+\alpha_4)/2 \qquad \bar{\alpha}_2 = (\alpha_1+\alpha_4)2$

and section 1 is upstream of the contraction, section, section 3 is at the vena contracta, section 4 downstream of the contraction, section 5 is upstream of the expansion and section 6 is downstream of the expansion. The notation does not become more compact by use of this summation since, for the general case, it is not known whether the expansion or contraction is upstream and no general rule for equality of α's can be assumed.

Fig. 6 compares the previously obtained U.C. data and those of Janssen[2] to total pressure loss predictions obtained from equation (7) using equation 5 for estimation of α_3 and using Hughmark's correlation[13] for α elsewhere. It is seen that reasonable agreement is obtained. This serves to validate the approachs used to obtain the component pressure changes.

In view of the cumbersome nature of Equation (7), some simplification is desirable. This is accomplished by making use of the fact that the homogeneous model provides a reasonable approximation of the contraction pressure drop (see Fig. 5). When this approximation is used we have

$$\Delta P_L \simeq \frac{G^2}{\sigma^2 g_c \rho_1}\left\{\frac{\rho_1}{2}\left(\frac{x}{\rho_g}+\frac{(1-x)}{\rho_1}\right)\left[\left(\frac{1}{C}-1\right)^2+(1-\sigma)^2\right]-\right.$$

$$\left.\sigma^2\left(\frac{\rho_1}{\rho_g}x^2\left(\frac{1}{\alpha_1\sigma}-\frac{1}{\alpha_2}\right)\right]-\sigma^2\left[(1-x)^2\left(\frac{1}{\sigma(1-\alpha_1)}-\frac{1}{(1-\alpha_2)}\right]\right\} \qquad (8)$$

where α_1 = void fraction upstream of expansion

α_2 = void fraction downstream of expansion

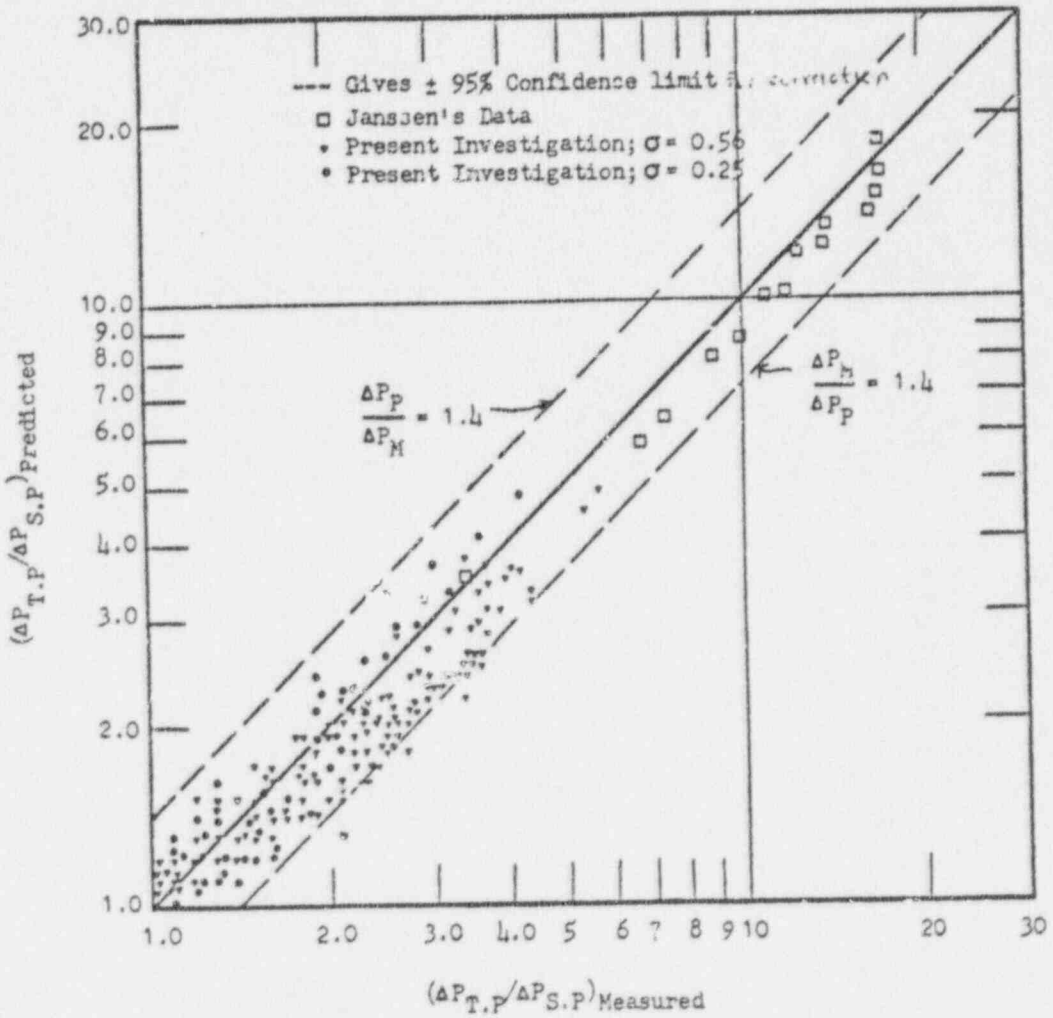

Fig. 6 Comparison of Measured Ratio of Two-Phase to Single-Phase Pressure Loss Across a Long Contraction-Expansion Section With the Ratio Predicted by Equation (7)

3.0 State of Art at Outset of Present Program

3.1 Well Separated Abrupt Area Changes

At the outset of the current program two-phase pressure drop across well separated abrupt area changes appeared to be fairly well understood. The one-dimensional momentum balance approach, coupled with appropriate estimation of α, leads to good predictions of available data. Predictions appear to be valid in both freon and steam-water systems with pressure ranging from 30 to 70 psia for Freon systems and from 55 to 1200 psia for water systems. Void fractions examined went from zero to over 90%. The mass velocity range over which test data is available is limited to the range from $G = 4 \times 10^5$ to $G = 2.5 \times 10^6$ lb/hr ft^2 (based on small size pipe).

A major question which remained unanswered was the determination of the conditions under which well separated behavior no longer applied.

3.2 Restrictions

When the restriction is of appreciable length, the abrupt area changes are well separated. The total pressure drop may then be obtained from Equation (7) providing vaporization is negligible. However, some economy of notation is possible since the outlet of the contraction is the inlet to the expansion. If we refer to the positions indicated in Fig. 7 we obtain

$$\Delta P_L = \frac{G_1^2}{2\rho_1 g_c}\left[\frac{1}{\sigma^2}\left\{\frac{\rho_1}{\rho_g}x^2\hat{a}_1\left(\frac{1}{C^2\alpha_3^2}-\frac{1}{\alpha_4^2}\right)+(1-x)^2(1-\hat{a}_1)\right.\right.$$
$$\left.\left(\frac{1}{C^2(1-\alpha_3)^2}-\frac{1}{(1-\alpha_4)^2}\right)\right\}-\frac{2}{\sigma^2}\left\{\frac{\rho_1}{\rho_g}x^2\left(\frac{1}{C\alpha_3}-\frac{1}{\alpha_4}+\frac{\sigma}{\alpha_4}-\frac{\sigma^2}{\alpha_5}\right)\right.$$
$$+(1-x)^2\left(\frac{1}{C(1-\alpha_3)}-\frac{1}{(1-\alpha_4)}+\frac{\sigma}{(1-\alpha_4)}+\frac{\sigma^2}{(1-\alpha_5)}\right)\Big\}+\frac{\rho_1}{\rho_g}x^2\hat{a}_2\left(\frac{1}{\sigma^2\alpha_4^2}\right.$$
$$\left.\left.-\frac{1}{\alpha_1^2}\right)+(1-x)^2(1-\hat{a}_2)\left\{\frac{1}{\sigma^2(1-\alpha_4)^2}-\frac{1}{(1-\alpha_1)^2}\right\}\right] \qquad (9)$$

Figure 7

(a) Long Insert

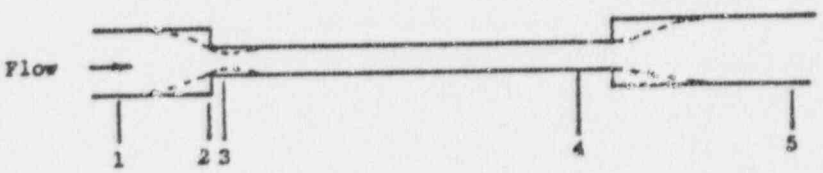

(b) Short Insert

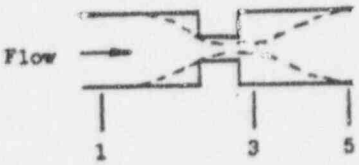

(c) Location of Pressure Taps

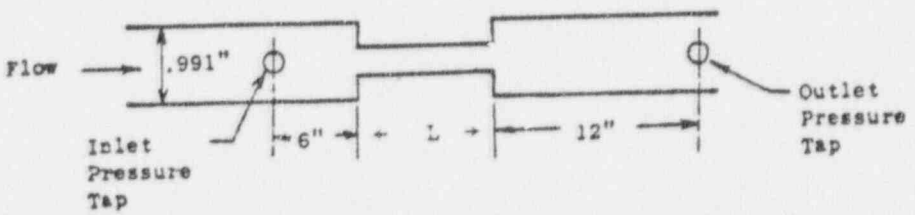

Value of L listed on p. 27

Janssen[2] obtained the same result by a slightly different approach. By subtracting the Bernouli pressure change, he determined that, based on a one-dimensional momentum, balance, the irreversible loss across the expansion is given by

$$\Delta p_{e_{L-x}} = \frac{G_5^2 v_1}{2g_c \sigma^2}\left[\frac{v_g}{v_1} x^2 \hat{a}_{ex}\left(\frac{1}{a_4^2} - \frac{\sigma^2}{a_5^2}\right) + (1-x)^2(1-\hat{a}_{ex})\right.$$

$$\left(\frac{1}{(1-a_4)^2} - \frac{\sigma^2}{(1-a_5)^2}\right) - 2\sigma\left(\frac{v_g}{v_1} x^2\left(\frac{1}{a_4} - \frac{\sigma}{a_5}\right)\right.$$

$$\left.\left. + (1-x)^2\left(\frac{1}{1-a_4} - \frac{\sigma}{1-a_5}\right)\right)\right] \qquad (10)$$

Similiarly, the contraction loss is given by

$$\Delta p_{cL-x} = \frac{G_1^2 v_1}{2g_c \sigma^2}\ \frac{1}{C^2}\left[\frac{v_g}{v_1} x^2\ \hat{a}_{c_x}\left(\frac{1}{a_3^2} - \frac{C^2}{a_4^2}\right)\right.$$

$$+ (1-x)^2(1-\hat{a}_{cx})\left(\frac{1}{(1-a_3)^2} - \frac{C^2}{(1-a_4)^2}\right) - 2C\left(\frac{v_g}{v_1} x^2\left(\frac{1}{a_4}\right.\right.$$

$$\left.\left.\left. - \frac{C}{a_4}\right) + (1-x)^2\left(\frac{1}{1-a_3} - \frac{C}{1-a_4}\right)\right)\right] \qquad (11)$$

where

$$\hat{a}_{ex} = (a_4+a_5)/2$$

and

$$\hat{a}_{cx} = (a_3+a_4)/2$$

Summation of Equations (10) and (11) yields Equation (9)

When very short inserts (orifices) are considered, a revised momentum balance is required since the vena contracta is outside the insert. (See Figure 7b) Based on a one dimensional momentum balance, Janssen[2] proposed that the pressure loss be obtained from

$$\Delta P_L \left(\begin{matrix}\text{SHORT}\\ \text{INSERT}\end{matrix}\right) = \frac{G_1^2 v_1}{2g_c\sigma^2}\frac{1}{C^2}\left[\frac{v_g}{v_1}x^2\hat{\alpha}_3\left\{\frac{1}{\alpha_3^2}-\frac{\sigma^2C^2}{\alpha_5^2}\right\}\right.$$

$$+(1-x)^2(1-\hat{\alpha}_3)\left\{\frac{1}{(1-\alpha_3)^2}-\frac{\sigma^2C^2}{(1-\alpha_5)^2}\right\}$$

$$\left.-2\sigma C\left\{\frac{v_g}{v_1}x^2\left(\frac{1}{\alpha_3}-\frac{\sigma C}{\alpha_5}\right)+(1-x)^2\left(\frac{1}{1-\alpha_3}-\frac{\sigma C}{1-\alpha_5}\right)\right\}\right] \qquad (12)$$

where $\hat{\alpha}_3 = (\alpha_3+\alpha_5)/2$ and the α's are void fraction locations as shown in Figure 1b.

The behavior of a very short insert is essentially that of an orifice and hence those models proposed for use with an orifice may be considered. Use of a simple homogeneous model is found to appreciably overestimate the pressure drop[12].

Murdock[13] arrived at a relatively simple expression making the assumptions of incompressible flow, negligible upstream momentum, no phase change, no interfacial shear forces and α constant across orifice. He obtained for the ratio of the two-phase pressure drop, (ΔP_{TP}), to the pressure drop which would be obtained with the gas phase alone (ΔP_g), was given by

$$\left(\frac{\Delta P_{TP}}{\Delta P_g}\right)^{0.5} = 1 + \left(\frac{\Delta P_g}{\Delta P_1}\right)^{0.5} \qquad (13)$$

where ΔP_l = pressure drop obtained with liquid phase flowing alone Murdock[13] found that his low quality steam water data were somewhat better correlated by a slightly modified equation

$$\left(\frac{\Delta P_{TP}}{\Delta P_g}\right)^{0.5} = 1 + (1.26)\left(\frac{\Delta P_g}{\Delta P_l}\right)^{0.5} \qquad (14)$$

Collier reports[14] that Chisholm followed an approach similar to that of Murdock[13] but allowed for interfacial shear. He obtained an expression of the form

$$\left(\frac{\Delta P_{TP}}{\Delta P_g}\right) = 1 + k\left(\frac{\Delta P_g}{\Delta P_l}\right)^{0.5} + \left(\frac{\Delta P_g}{\Delta P_l}\right) \qquad (15)$$

Chisholm and Leishman[15] suggest that k is a function of reduced pressure, P_r. Below a pressure of 150 bar, that suggest for steam-water mixtures

$$k = Z + \frac{1}{Z}$$

where $Z = 0.19 + 0.92\ P_r$

The correlation approaches of Chisholm and Murdock have the disadvantage of being inconsistent with the approach which has been successful in handling well separated expansions and contractions. On the other hand, the approach suggested by Janssen[2] which can allow for variation in α across the restriction, is consistent with the method found useful previously.

It should be noted that the pressure loss across a short insert is considerably higher than that for a long insert (ignoring pipe friction) of the same σ. This may be easily seen by considering single-phase behaviour. The single-phase pressure loss for a long insert is given by

$$\Delta p_L \left(\begin{matrix}\text{LONG}\\ \text{INSERT}\end{matrix}\right)_{1\phi} = \frac{G_1^2}{2g_c\rho_1\sigma^2}\left[1-2\sigma+\sigma^2+\frac{1}{C^2}-\frac{2}{C}+1\right] \tag{16}$$

The single phase pressure loss across a short insert, obtained from Eq. 12 by setting x and c at zero, is given by

$$\Delta p_L \left(\begin{matrix}\text{SHORT}\\ \text{INSERT}\end{matrix}\right)_{1\phi} = \frac{G_1^2}{2g\sigma^2\rho_1}\frac{1}{C^2}\left[1-2\sigma C+\sigma^2C^2\right] \tag{17}$$

It is found that if Equation 16 is subtracted from Equation 17 then

$$\Delta p_L \left(\begin{matrix}\text{SHORT}\\ \text{INSERT}\end{matrix}\right) - \Delta p_L \left(\begin{matrix}\text{LONG}\\ \text{INSERT}\end{matrix}\right) = \frac{G_1^2}{2g_c\rho_1\sigma^2}\left[\frac{2(1-C)(1-\sigma)}{C}\right] \tag{18}$$

In addition to the previously noted experimental work of James[12] and Murdock,[13] two-phase pressure losses across orifices and short inserts have been studied experimentally by Hoopes[16] and Cermatk et al[17]

Hoopes (16) investigated two phase losses through orifices in 1957 and determined that the best correlation between theory and experimental data was obtained when slip flow was assumed everywhere, including at the vena contracta. In 1966, Janssen[2] obtained similar results for very short inserts.

An investigation of short inserts was also made in 1964 by Cermak[17] et al. Their data did not agree with that of Janssen[2] or Hoopes[16], but Cermak et al[8] obtained their pressure drop readings at locations where complete recovery from the expansion had not yet occured. Therefore, their pressure drops may be expected to be larger than would be observed if they obtained their readings after complete recovery had occured.

The data of Hoopes[16] and Janssen[2] indicate that short insert behavior differs from long insert behavior in that little mixing occurs at the vena contracta in the short insert. However, none of the previous conditions address the question of when an insert may be considered long or short. Further, some sort of transition region may be expected and the behavior in this region had not been examined.

4.0 Test Program

4.1 Overall Plan

As the data available at the outset of the study indicated that the two phase pressure loss behavior of long and short inserts differed, a further investigation appeared warranted. The present study was designed to confirm these earlier observations and to explore the region where the change in behavior occurs.

Since a circulating Freon loop was available, the fluid used in these tests was Freon 113 (molecular wt. = 187.39, boiling point at atmospheric pressure = 117.5°F). Because of the low boiling temperature and the low heat of vaporization (59.5 BTU/lbm at 2 atm.) it was possible to test with a variety of pressure and flow rates while the heat addition requirements remained relatively low. Because Freon 113 has a high molecular weight, the Freon vapor densities were of the same order of magnitude as the steam in some nuclear reactor systems. All parameters cannot be simmulated and the ratio ρ_{ℓ}/ρ_g is higher in the Freon system than for steam-water.

Six test sections were examined in the loop using circulating Freon. These test sections spanned the region where the transition from long insert to short insert behavior accurred. It was then possible to determine the modifications to the one dimensional momentum balance model needed to predict the observed behavior.

4.2 Test Apparatus and Procedures

The boiling Freon loop used in the present tests is the same apparatus used by Husain and Weisman[1] in their tests of well separated expansions and contractions.

The loop used is shown schematically in Fig. 8. The main loop piping is $1\frac{1}{2}$" schedule 40 carbon steel. The liquid Freon is circulated by a 30 gpm centrifugal pump provided with a specially balanced seal to prevent Freon leakage. On leaving the pump liquid flows to a specially bored pipe section containing an orifice for flow measurement. (See Appendix for flow calculation details)

Freon vapor is generated in two vertical sections by means of electric immersion heaters (30 kw capacity). The two phase mixture then flows through the test section which contained some glass piping. A flexible hose at the end of the test section accommodates differential expansion.

The two-phase mixture leaving the test section proceeds to a water cooled condenser. The condensate returns to the pump inlet and is recirculated.

Pressure on the system is maintained by means of a large bladder type accumulator. The rubber diaphragm in the accumulator prevents contact between the Freon and the nitrogen used to maintain gas overpressure.

Test section pressure drops are measured by a multi range (0-10 to 0-168 in,water) bellows type differential pressure cell (Honeywell Model 29). Cooling jackets supplied with tap water assure that the lines to the differential pressure cell contain only liquid. Cooling jackets are also provided on the lines leading to the differential pressure cell measuring pressure drop across the orifice in the main liquid flow.

Two void meters were used during the tests. The downstream was used primarily to determine if vaporization was occuring across the test sections during the tests. If vaporization was occuring, then the pressure drop readings were corrected for the resulting acceleration losses incurred. The void sensors have been described in reference (1).

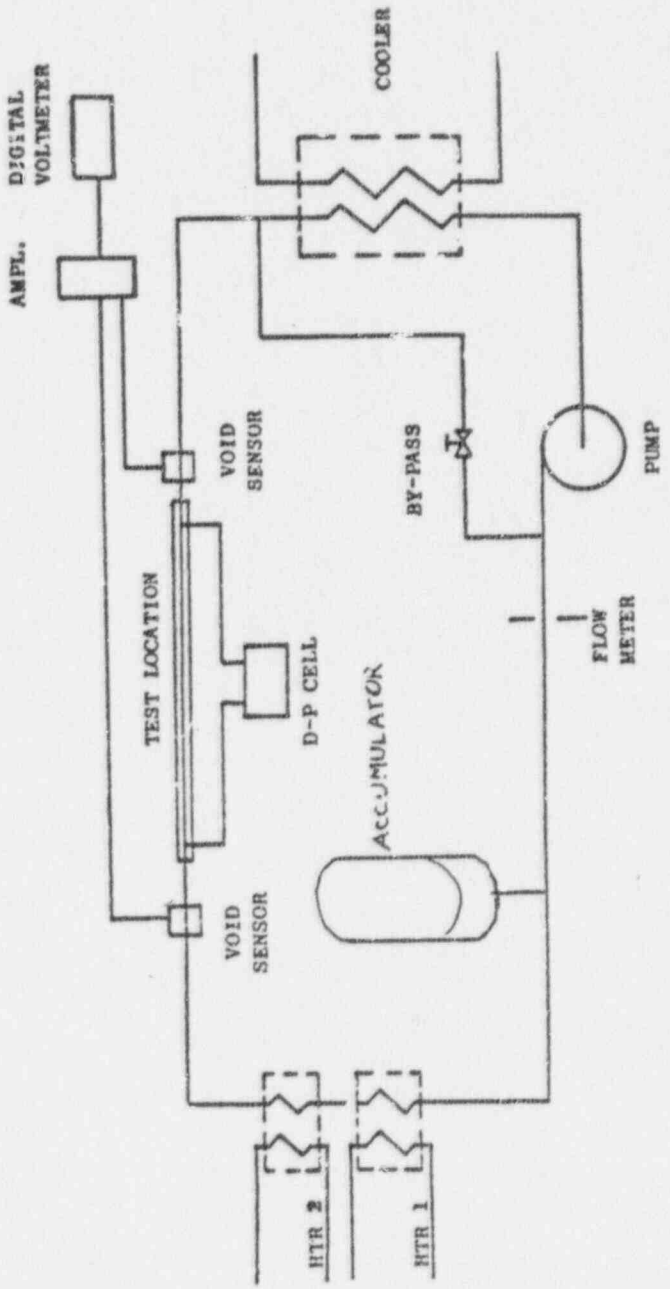
AMPL.
DIGITAL VOLTMETER
COOLER
VOID SENSOR
BY-PASS
PUMP
TEST LOCATION
D-P CELL
ACCUMULATOR
FLOW METER
VOID SENSOR
HTR 2
HTR 1

FIGURE 8

4.3 Test Program

Six restrictions were tested in this investigation. Dimensions of the test inserts are given in Table 2a and 2b. Each insert was tested over the range of pressures and mass flow rates indicated in Table 3. Glass pipe was immediately upstream and down stream of the horizontal test section to permit visual observation of flow patterns to and from the restriction.

Janssen's[2] previous study had indicated that a one-half inch long test section in a $\frac{1}{2}$ inch long channel behaved as a long insert while a .1 inch long insert in the same channel produced results like those of a thin orifice plate. It was decided to have a test section similar to each of these Janssen inserts[2] (S-2 & S-1 respectively) so as to verify these results. These are the test sections indicated by TS-1 and TS-3 in Table 2a. Two test sections of the same length but with different restriction diameters were then needed to determine the effect of restriction diameter on the results. The lengths of the sections were chosen so as to be in the transition region. These are sections TS-2 and TS-6 in Table 2a.

In the interest of generality, the behavior effect of multi-hole restrictions was investigated. Two inserts, having area ratios within the range examined with single-hole inserts, were chosen. Both inserts contained 4 holes of equal diameter. One insert was approximately the same length as the single hole thick orifice (TS-3), while the second was approximately the same length as the two single-hole restrictions in the transition region (TS-2 & TS-6). These are indicated as TS-4 & TS-5 in Table 1b. The 4 holes in these restrictions were placed on a ~7/16" pitch and were equidistant from the center of the large pipe.

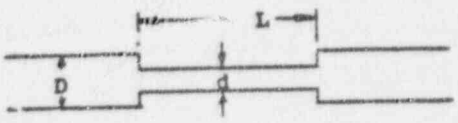

TABLE 1 (a)

DISCRIPTION OF SINGLE-HOLE TEST SECTIONS

INSERT NO.	MATL.	d INCHES	D INCHES	L INCHES	FLOW AREA RATIO σ
TS-1	GLASS	.761	.991	2.0	.590
TS-2	TEFLON	.764	.991	.505	.595
TS-3	STL.	.777	.991	.215	615
TS-6	STL.	.495	.991	.520	.249

TABLE 2 (b)

DISCRIPTION OF MULTI-HOLE TEST SECTIONS

INSERT NO.	MATL.	NO. OF HOLES	d* INCHES	D INCHES	L INCHES	FLOW AREA RATIO σ
TS-4	STL	4	.352	.991	.189	.505
TS-5	STL	4	.362	.991	.617	.534

*d for multi-hole inserts is the diameter of a single hole

The test conditions used are summarized in Table 3. The details of the experimental procedure used are provided in the appendix.

4.4 Experimental Results

Examination of the void fraction measurement indicated good agreement between the inlet and outlet void fraction readings at the lower flow rates. At flow rates above approximately 2.5×10^6 lbm/hr ft^2 within the restriction, a higher outlet void fraction was noted resulting in an acceleration pressure drop. The effect increased with increasing void fraction. When the flow was less than 3×10^6 lbm/hr ft^2 and the average void fraction was about 50%, the difference between the inlet and outlet readings were within 3% of the average value. If the void fraction was less than 30%, no significant difference was found between the inlet and outlet void fraction. When the flow rate through the restriction was 4.6×10^6 lbm/hr ft^2, it was found that the difference between the inlet and outlet void fraction was over 20% when the average void fraction was only 35%. This was considered excessive and therefore no data at mass velocities above 3×10^6 lbm/hr ft^2 (based on the restriction flow area) was used for evaluation of test section performance.

The acceleration losses were calculated in the standard manner [18]

$$\Delta p_a = \frac{G_1^2}{g_c}\left[\frac{(1-x_e)^2}{1-\alpha_e} v_l + \frac{x_e^2}{\alpha_e} v_g - \frac{(1-x_i)^2}{1-\alpha_i} v_l - \frac{x_i^2}{\alpha_i} v_g\right] \qquad (19)$$

where α_i, α_e = inlet and exit void fractions, respectively

x_i, x_e = inlet and exit qualities, respectively (Calculated from measured α using Hughmark's correlation)

It is seen from the tables in Appendix B that the acceleration pressure loss is generally a small percentage (10%) of the total loss. A sample calculation is found in Appendix B.

TABLE 3

DISCRIPTION OF TEST CONDITIONS

INSERT NO.	RANGE OF PRESSURES PSIG	RANGE OF MASS FLOW RATES RESTRICTION lbm/hr Ft^2	LARGE PIPE lbm/hr ft^2
TS-1	25-60	$2.0x10^6$-$2.8x10^6$	$1.2x10^6$-$1.6x10^6$
TS-2	40-60	$1.9x10^6$-$2.4x10^6$	$1.2x10^6$-$1.4x10^6$
TS-3	25-60	$1.9x10^6$-$2.7x10^6$	$1.2x10^6$-$1.6x10^6$
TS-4	25-60	$2.3x10^6$-$2.8x10^6$	$1.2x10^6$-$1.4x10^6$
TS-5	25-60	$2.2x10^6$-$2.7x10^6$	$1.2x10^6$-$1.4x10^6$
TS-6	25-60	$2.1x10^6$-$4.6x10^6$	$.5x10^5$-$1.1x10^6$

The measured pressure drop included the frictional losses in the pipe and test section between the upstream and downstream taps as well as the loss due to the restriction itself. The frictional loss is subtracted from the observed loss to obtain the loss due to the area change. In obtaining the pipe friction the Baroczy[17] correlation was used for the estimation of the two-phase friction multiplier.

A third correction to the measured pressure drop was necessary at some of the void fractions. Based on Mendler's[4] data for pressure drop across an abrupt expansion, it appears that, at high void fractions, the downstream pressure tap (12 inches from the expansion) is located before full pressure recovery from the expansion occurs. Mendler's[4] data for Δp versus distance from the expansion were obtained with a 1 inch diameter pipe. Since the test sections used in this investigation were placed in a one inch pipe, the fraction of the pressure drop which remained unrecovered at the tap location was based on Mendler's[4] data. Figure 9 shows the correction curve used and Appendix E details the technique used to arrive at this curve.

The experimental data and the corrections for various effects are given in the tables in Appendix C. A sample calculation is also provided in Appendix B.

The corrected ratio of the two-phase to the single phase pressure loss across the area change is plotted versus the average of the inlet and outlet void fraction (α) in Figures 10-15. The vertical and horizontal lines thru the data indicate the estimated error range (2σ). The error analysis is given in Appendix D.

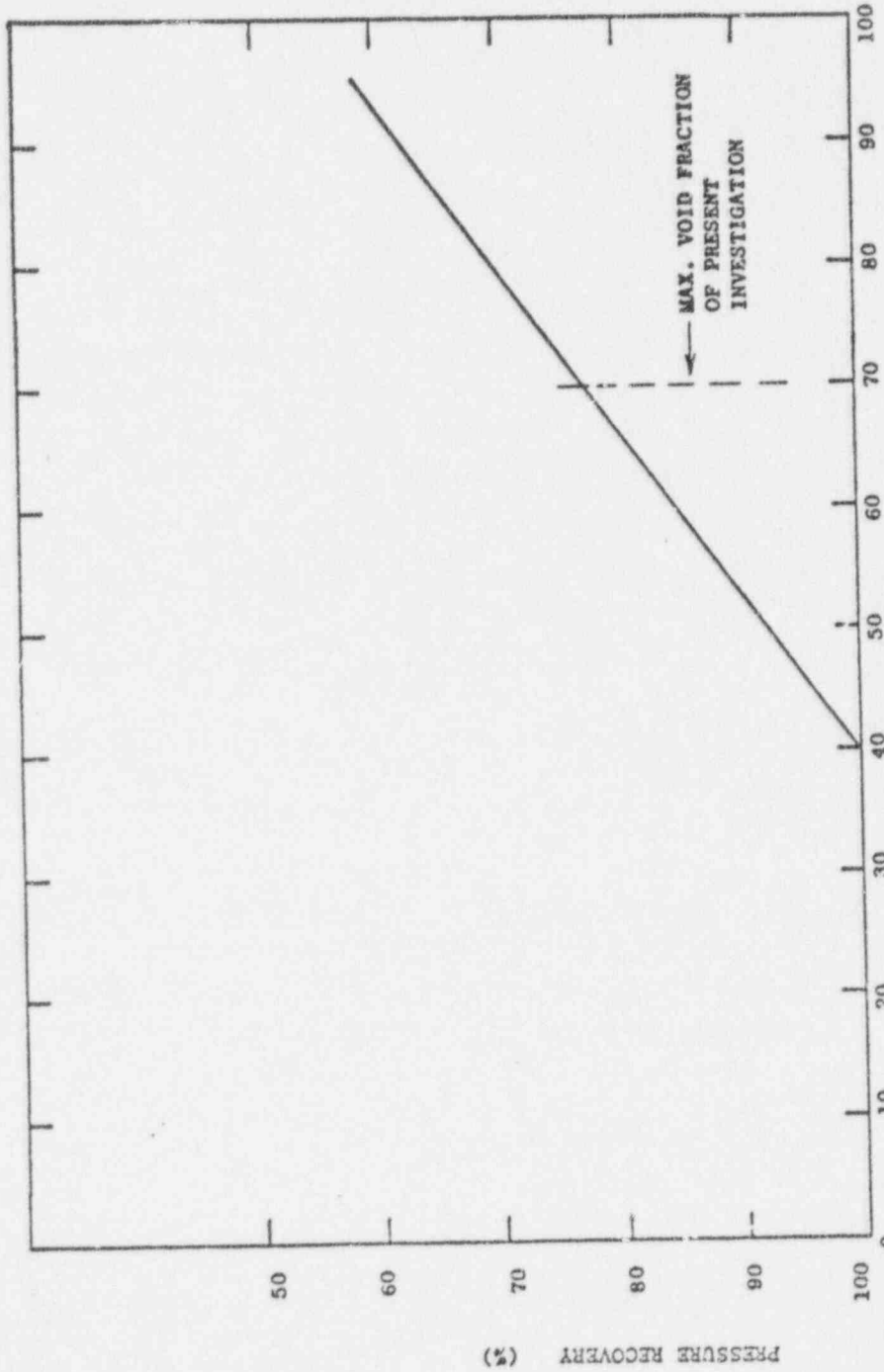

FIG.9 PRESSURE RECOVERY vs VOID FRACTION 12 INCHES FRO XPANSION

The lowest of the two solid lines in Figures 10-15 is the pressure loss ratio predicted assuming slip flow everywhere. The upper solid line is the predicted pressure loss ratio assuming slip flow everywhere except at the vena contracta where homogeneous flow is assumed. These lines are the upper and lower limits of the pressure loss ratio and are discussed in detail in Section 3.1 of this report. The dashed line which appears in Figures 11, 14, and 15 is a visual estimation of the mean line through the experimental data.

From Figures 10-15, it is seen that, though a range of pressures and flows were used for each test section, the data for any one test section produced a trend that was independent of the pressure and the flow rate through the restriction. For example in Figure 15, the path of the data at 25 PSIG and 2.1×10^6 lbm/hr ft^2 is the same path for the data at 60 PSIG and 2.9×10^6 lbm/hr ft^2.

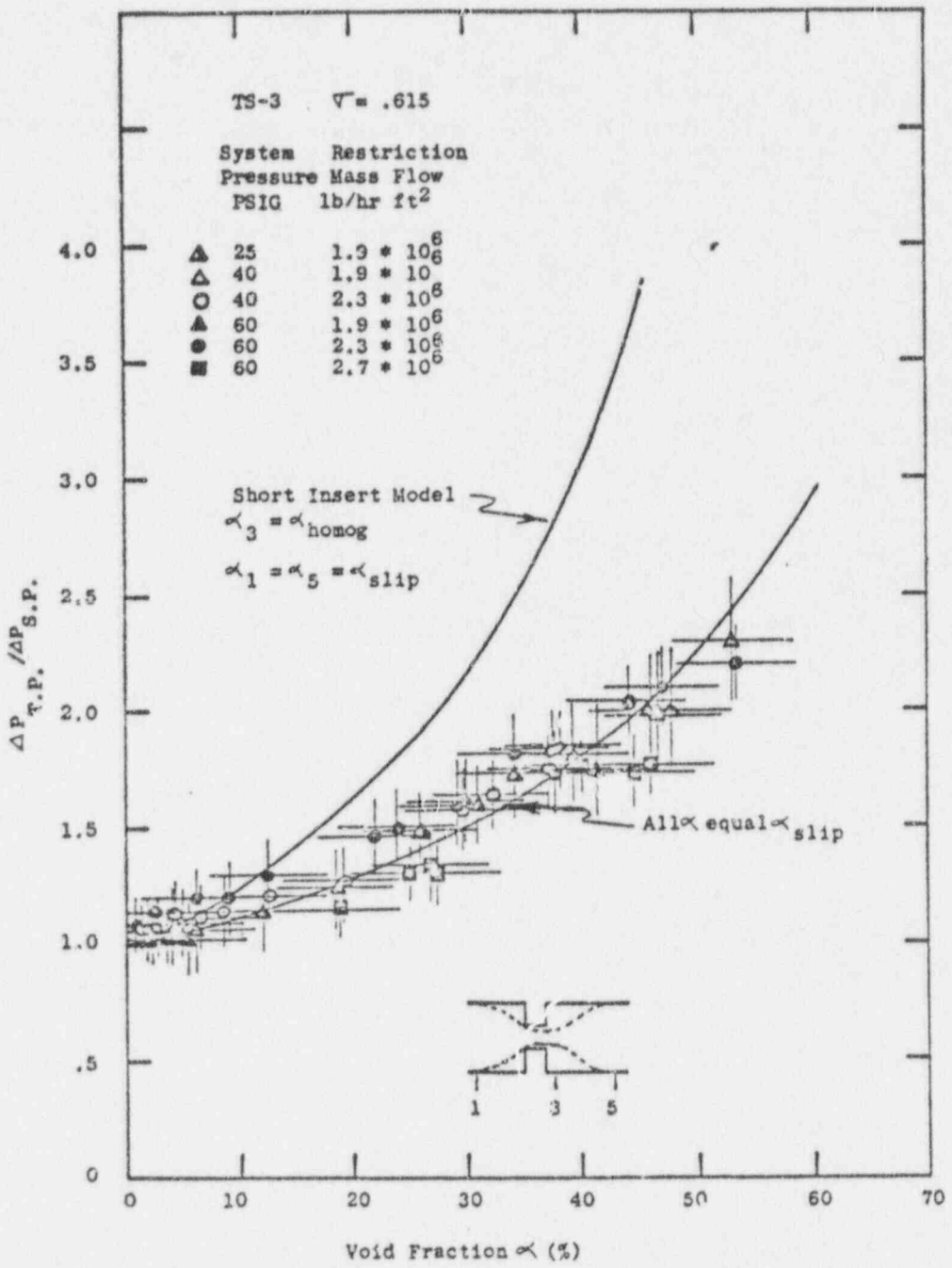

Figure 10 Ratio of Two Phase to Single Phase Pressure Drop Across an Abrupt Restriction .215 Inches Long

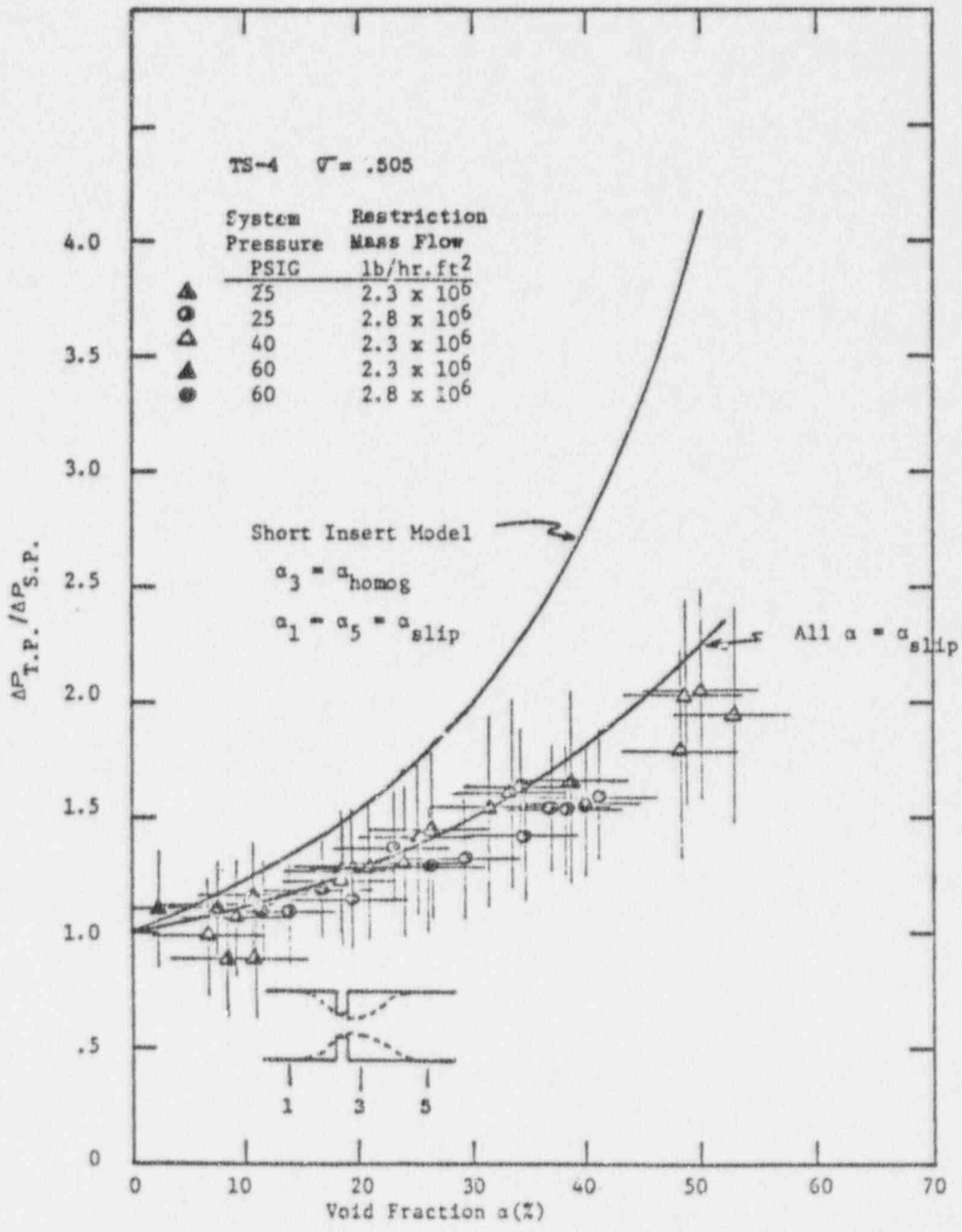

Figure 11 Ratio of Two Phase to Single Phase Pressure Drop Across an Abrupt 4 Hole Restriction .189 inches Long

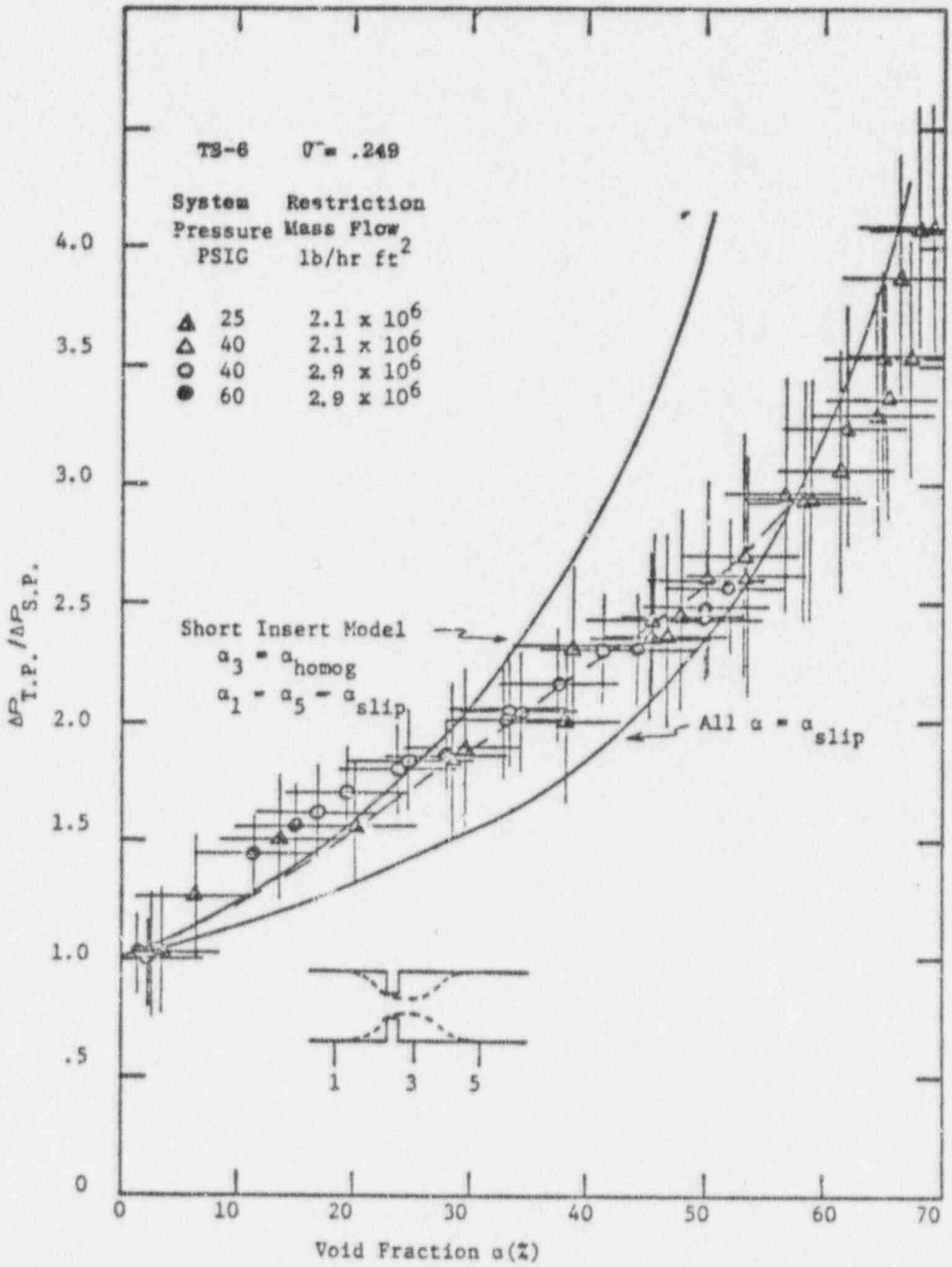

Figure 12 Ratio of Two Phase to Single Phase Pressure Drop Across an Abrupt .495 Inch Diameter Restriction .520 Inch Long

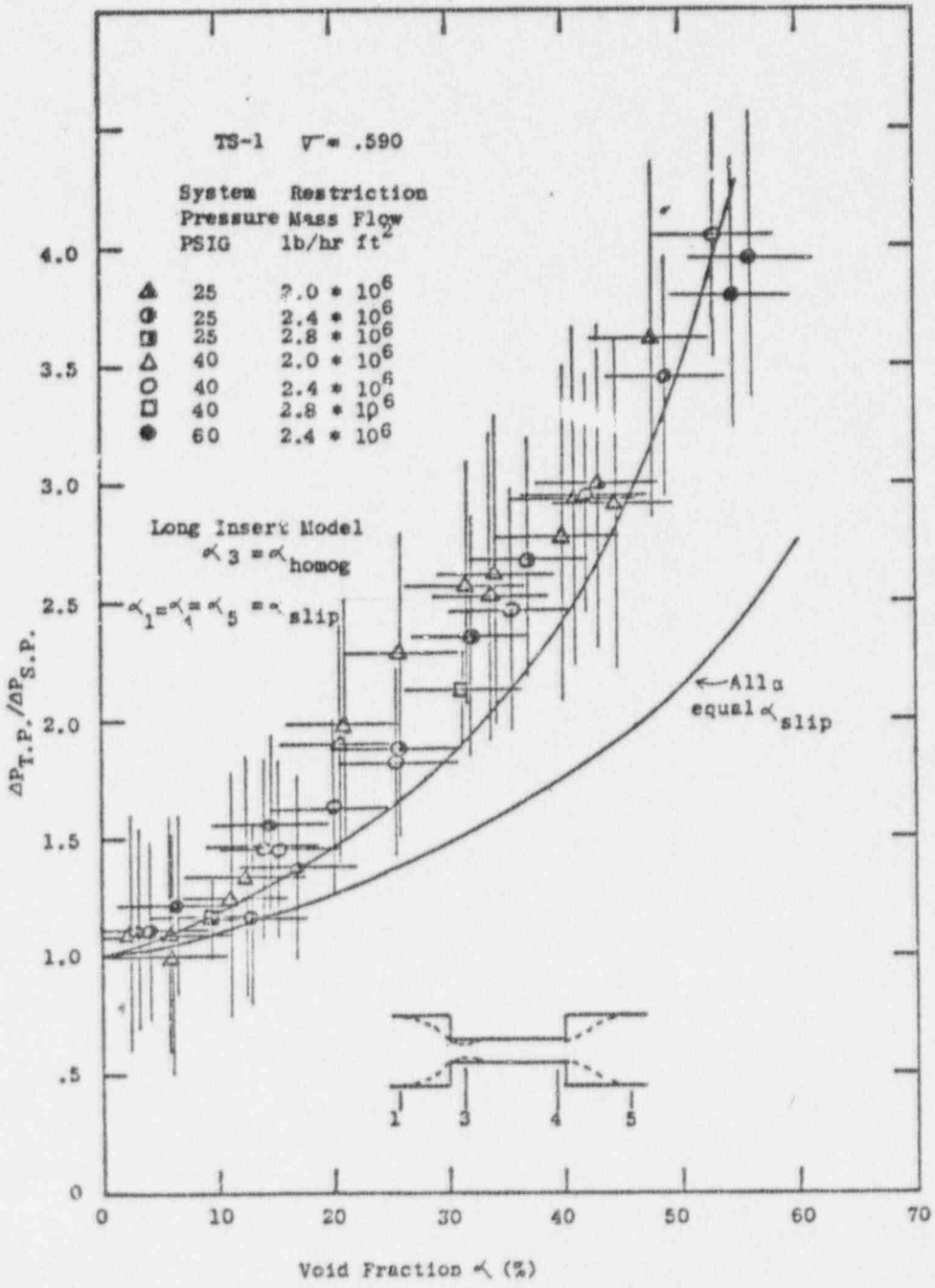

Figure 13 Ratio of Two Phase to Single Phase Pressure Drop Across an Abrupt Restriction 1.0 Inches Long

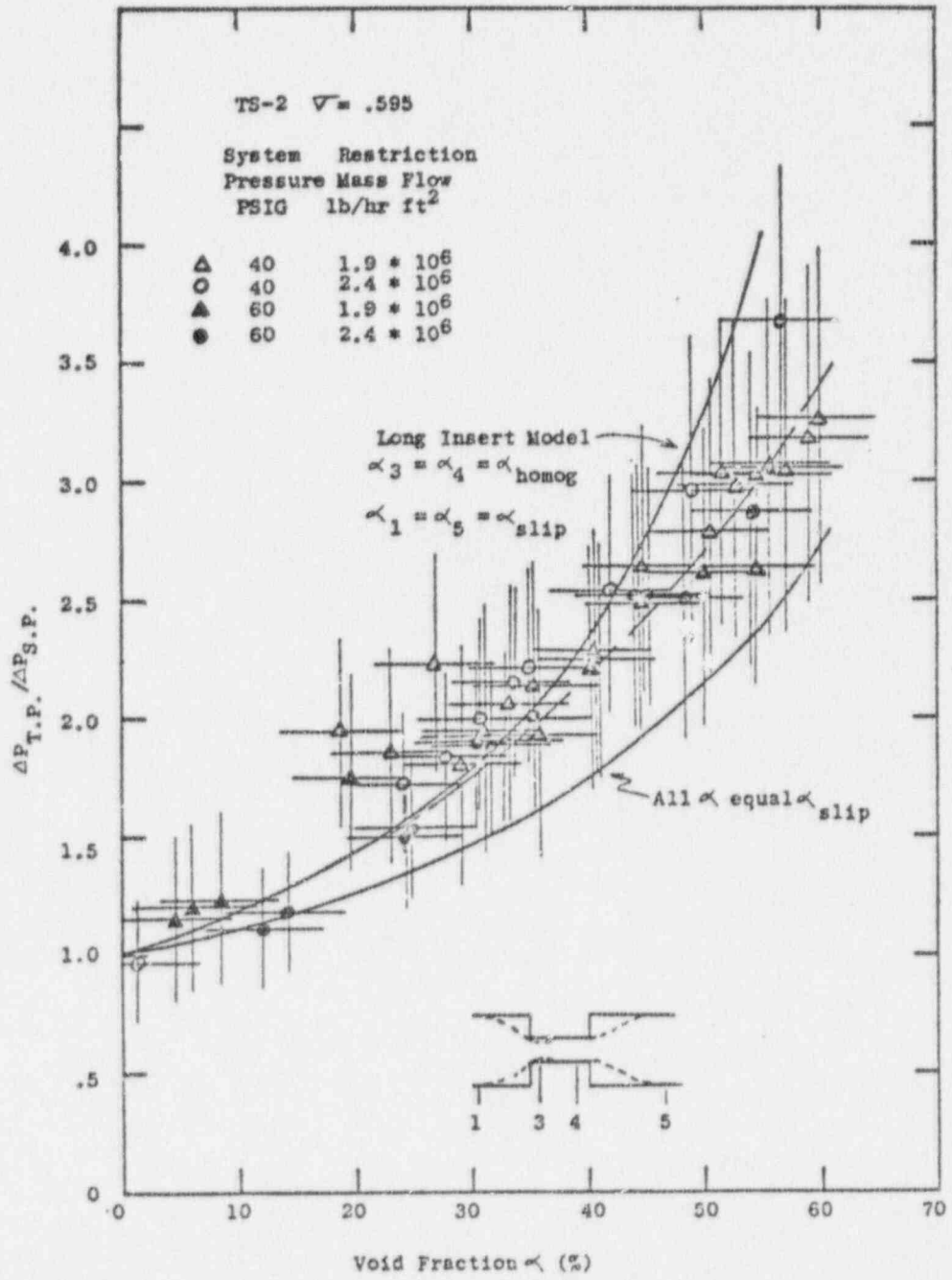

Figure 14 Ratio of Two Phase to Single Phase Pressure Drop Across an Abrupt Restriction .505 Inches Long

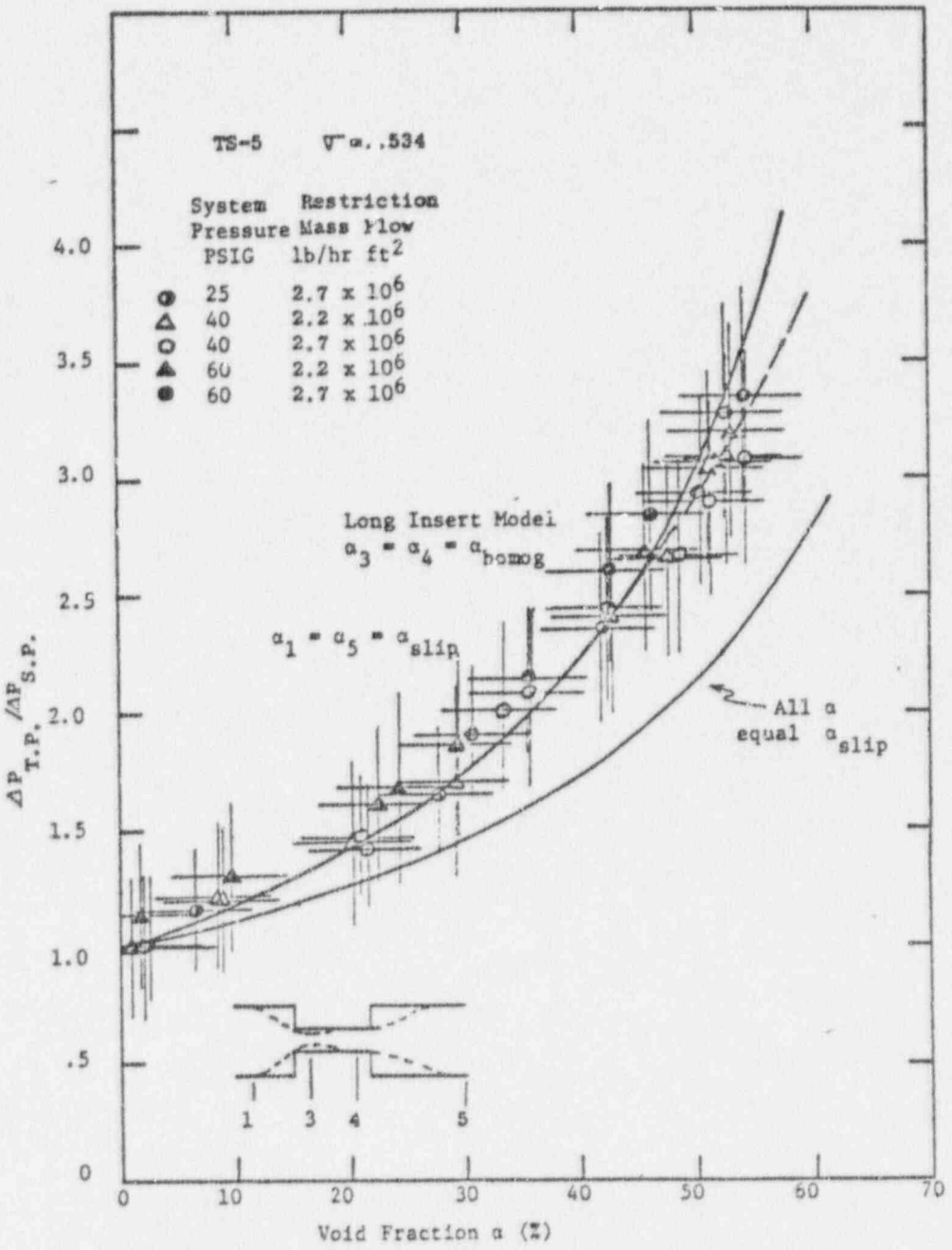

Figure 15 Ratio of Two Phase to Single Phase Pressure Drop Across an Abrupt 4 Hole Restriciton .617 Inches Long

5.0 Analysis of Results

5.1 Comparison of Results with Previous Correlations

It has been previously observed that the pressure loss equation which should be used (Equation 8 or 11) for prediction of two-phase pressure drop across a restriction depends on whether the vena contracta occurs within or without the restriction. The ASME Fluid Meters[20] estimate of the position of the vena contracta downstream of an orifice was used for this determination (see Fig. 16). For a given restriction diameter to large pipe diameter ratio, the mean line of Fig. 16 was used to decide whether the long insert equation (Eq. 8) or the short insert Equation(12) should be used.

The applicability of the model chosen to the particular insert was confirmed by examination of the single phase data. These data were used to compute C the value of the vena contracta area ratio (by use of Eq. 13 or 14). In all cases reasonable value of C ($-6 \leq C \leq .75$) were obtained. When the incorrect momentum balance is used values of C outside of the expected range are obtained. Further details of this computation, including the values of C obtained, are given in the Appendix.

The single-phase behavior sections TS-3, TS-4 and TS-6 was found to be described by the short insert momentum balance equation. These data were then compared to equation (12) making two distinct assumptions; viz:

a) The void fractions α, at all locations is equal to the measured value and that quality, x, is related to α by Hughmark's[8] slip flow correlation

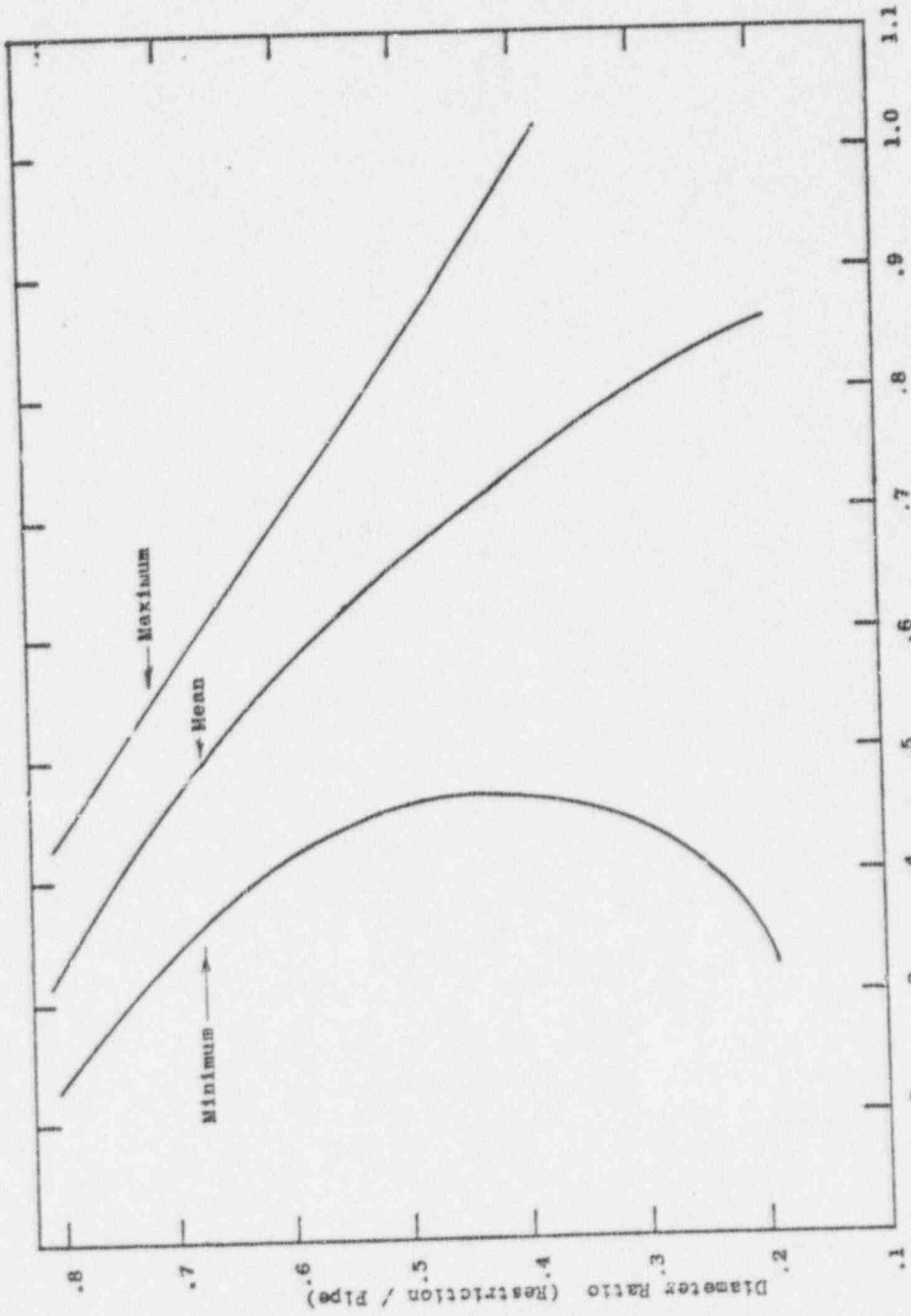

Figure 16 Position of Minimum Static Pressure Downstream of Orifice

$$\frac{1}{x} = 1 - \frac{\rho_l}{\rho_g}\left(1 - \frac{K}{\alpha}\right) \tag{17}$$

where K is a function of Z and $Z = (Re)^{1/6}(F_r)^{1/8}(1-\alpha)^{-1/4}$

or

b) The upstream and downstream void fractions are the measured values and x is obtained as in (a). The void fraction at the vena contracta is assured to be that for homogeneous flow and is obtained for X run

$$\alpha_h = \frac{x}{x + (1-x)(\rho_g/\rho_l)} \tag{18}$$

The results of these comparisons are seen in Figs 10, 11, and 12. While TS-3 and TS-4 follow the curve calculated from assumption (a), TS-6 shows higher pressure drops over a wide range of void fractions.

The single-phase behavior of TS-1, TS-2 and TS-5 were described by the long insert pressure drop equation. The data obtained from TS-1 were compared to Equation (8) using the assumption of both (a) and (b) given above. A slightly different procedure was used for TS-2 and TS-5 which had short insert lengths (.505 in and .99 in respectively). Here, one comparison was based on the assumption of set (a) but assumption set (b) was modified. In view of the short length of these restrictions it seems unreasonable to assume complete mixing at the vena contracta and reversion to slip flow just upstream of the expansion From the mean line of Fig. 16 it may be seen that the vena contracta occurs about 0.4 in downstream of the restriction inlet.

Hence only $\simeq$ 0.1 inch remains before the expansion occurs. For this reason, when mixing at the vena contracta of TS-2 and TS-5 was assumed, the void fraction just upstream of the expansion was taken to be identical to that at the vena contracta. Visual observations made with these test sections appeared to confirm these assumptions.

Examination of the experimental results for test sections 1, 2 and 5, (plotted in Fig. 13-15) shows them to be clearly different than these for test sections classified as short insert. The observed pressure drops for the short inserts clustered about the curves obtained assuming all α equal α_{slip}. The long insert data, on the other hand, tend to cluster around the curve obtained taking $\alpha = \alpha_{homg}$ at the vena contracta. However, both TS-2 and TS-5 show somewhat lower values than predicted by the curve at the higher void fractions.

5.2 Mixing Factor Determination

In the foregoing, section, it was observed that the test results tended to be somewhere between the predictions for all slip flow and there for full mixing, at the vena contracta. This suggests that the mixing factor concept, used for high void data in an abrupt contraction, (see Equation 5) could be expanded. If we assume that the difference in observed behavior is due to variations in the degree of mixing at the vena contracta, then, following Equation 5, we may write,

$$\alpha_3 = \alpha_{slip} + A(\alpha_{homogeneous} - \alpha_{slip}) \qquad (19)$$

where A is a mixing factor which depends on void fraction and test section geometry. The validity of this approach was confirmed by visual observation of the short inserts. Both TS-3 and TS-4 showed very little mixing at the insert outlet.

The mixing behavior of two of the short inserts is shown in the photographs of Fig. 17. Figures 17a, b, and c are of test section TS-3 while Fig. 17d and e are TS-6. We note that Figs 17a and c show that the flow is not mixed at the test section outlet. This observation is in accord with the pressure drop observations which agree with the assumption of no mixing at the vena contracta.

The photographs of TS-6 at low α, shown in Fig. 17d, and e show a different behavior. Here rather complete mixing is seen at the outlet. This again is in accord with the pressure drop observations which, at low voids, are in agreement with the pressure drop calculated by assuming vena contracta mixing.

In view of the foregoing, values of the mixing factor, A, were determined for each of the inserts studied. In making these calculations, the assumptions outlined in the previous section were used. Thus, the short insert momentum balance model was used for test sections 3, 4 and 6. The long insert momentum balance was used for test sections 1, 2 and 5. As previously, the void fraction at the vena contracta and exit were taken to be the same in test sections 2 and 5.

Values of the mixing factor were determined by a trial and error procedure. The value of α_3 was varied until the predictions agreed with the mean of line through the data at a given α. The corresponding value of A was then obtained from Equation (18).

The mixing factors obtained for the various inserts examined are shown in Tables 4a and 4b. The single hole insert that behaves as a long insert (TS-2) is seen to have mixing factors that start at unity and become smaller as the void fraction increases. The two single hole inserts, whose losses are predicted by the short insert equation

Figure 17

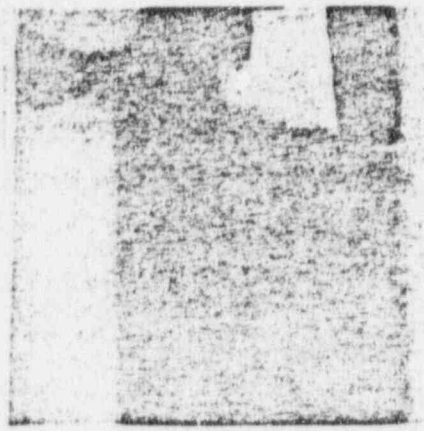

(a) Outlet TS-3
$G = 1.9 * 10^6$ lb/hr ft^2
$\alpha \leq 10\%$

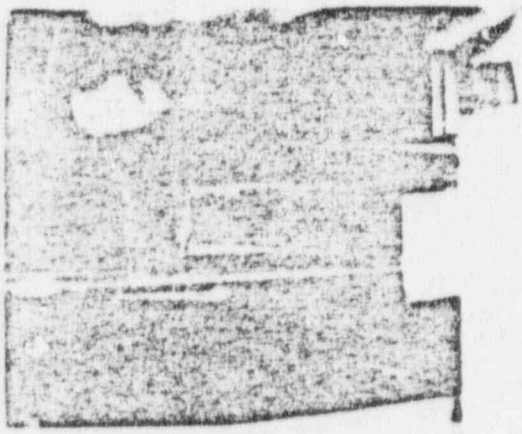

(b) Inlet TS-3
$G = 1.9 * 10^6$ lb/hr ft^2
$\alpha \leq 10\%$

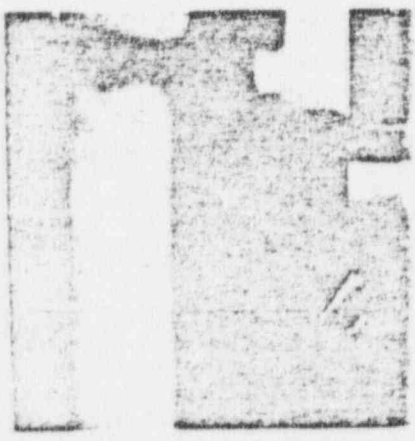

(c) Outlet TS-3
$G = 1.9 * 10^6$ lb/hr ft^2
$\alpha \leq 10\%$

Figure 17 (cont.)

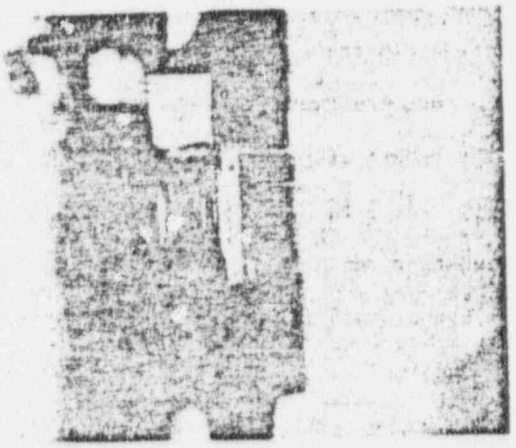

(d) Outlet TS-6
G = 2.1 * 10^6 lb/hr ft^2
$\alpha \leq 10\%$

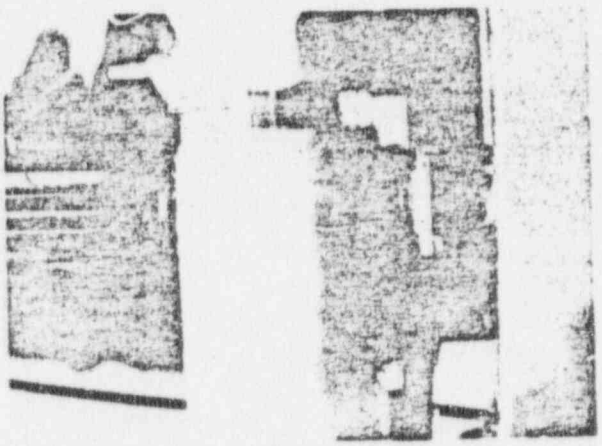

(e) Inlet and Outlet TS-6
G = 2.1 * 10^6 lb/hr ft^2
$\alpha \leq 10\%$

(TS-3 and TS-6), indicate, as previously noted, that for very short inserts no mixing at the vena contracta occurs, while for longer restrictions some mixing is found. In the latter case, the mixing decreases rapidly with increasing void fraction.

The data for the two 4-hole restrictions in Table 4b are found to be consistent with the single hole restriction data. For the short restriction, where the vena contracta occurs outside the restriction (TS-4), no mixing at the vena contracta occurs. This is consistant with the data for the very short single hole restriction. For the long 4-hole restriction (TS-5), where the vena contracta occurs within the restriction, it was found that the mixing at the vena contracta was complete, except at the higher void fractions. At the high void fraction values, the mixing tends to decrease at a rather slow rate. This observation is consistant with the single hole restrictions where the vena contracta occurs within the restriction.

5.3 Correlation of Mixing Factors

The variation of the mixing factors shown in Table 4 indicate that these are both void fraction and geometry effects. Several possibilities have been considered as the appropriate geometric variables - One such possibility is the distance between the upstream (contraction) face and the vena contracta. However, inspection of Table 4 clearly shows that test sections having similar values for this parameter have different mixing factors.

The length of the insert alone is not an adequate correlating variable since test sections with very nearly the same length (e.g. TS-2 and TS-6) show decidedly different mixing. Mixing appears to increase with restriction length and to decrease with restriction diameter.

TABLE 4 (a)

MIXING FACTORS FOR SINGLE HOLE RESTRICTIONS

INSERT NO.	VOID FRACTION %	MIXING FACTOR	LENGTH OF INSERT INCHES	LENGTH - CONTRACTION FACE 1 TO VENA CONTRACTA INCHES
TS-1	0-60	1.00	2.0	∿.37
TS-2	0-20	1.00	.505	∿.37
	40	.74		
	50	.60		
	60	.40		
TS-3	0-60	.00	.215	∿.37
TS-6	20	.90	.520	∿.65
	30	.65		
	40	.45		
	50	.17		
	≥ 60	.00		

TABLE 4 (b)

MIXING FACTORS FOR MULTI-HOLE RESTRICTIONS

INSERT NO.	VOID FRACTION %	MIXING FACTOR	LENGTH OF INSERT INCHES	LENGTH CONTRACTION FACE TO VENA CONTRACTA INCHES	NO. OF HOLES
TS-4	0-60	.00	.189	∿.42	4
TS-5	0-40	1.00	.617	∿.43	4
	50	.90			
	60	.70			

Figure 18 shows the mixing factors as a function of the ratio $L/d_{restriction}$ The data all appear to be consistent with this approach.

Note that the data obtained for multiple hole inserts (TS-4 and TS-5) are consistent with the remaining data providing $d_{restriction}$ is taken as the diameter of an individual hole.

Figure 18 also includes data by Janssen[2] on inserts of several lengths. These data which are either for very short inserts or relatively long inserts (see table 5 for insert geometry) and hence show mixing factors of zero or one. The data of Janssen[2] appear to be consistent with the data of the present investigation.

Two phase pressure drops across short inserts have also been investigated by Cermak et al.[4]. However, their pressure taps were very close to the insert (.7 in downstream). Both the data of Janssen and Kervinen[8] and Mendler[6] indicate that only a fraction of the expansion pressure rise would not be seen so close to the area change. Interpretation of this data is clouded by the fact that the degree of recovery close to such an insert is a function of void fraction and mean velocity as well as distance from the insert.

In the range of mass flows for which non-recovery effects could be estimated from Janssen and Kervinens work[6] prediction based on the present correlations were compared with Cermak's data. Reasonable agreement is attained. Cermak's data show lower ratios of 2 phase to single phase pressure drop at the lower mass flows ($G < 75 \times 10^6$ lbs/hr ft^2 through the restriction) but non-recovery effects at these flows cannot be estimated and no conclusions can be drawn from the data.

The data obtained in the present investigation agree with Hoope's [16] conclusion that orifice pressure drops should be calculated using slip

Fig. 18 Mixing Factor (A)
vs
Length/Restriction Diameter

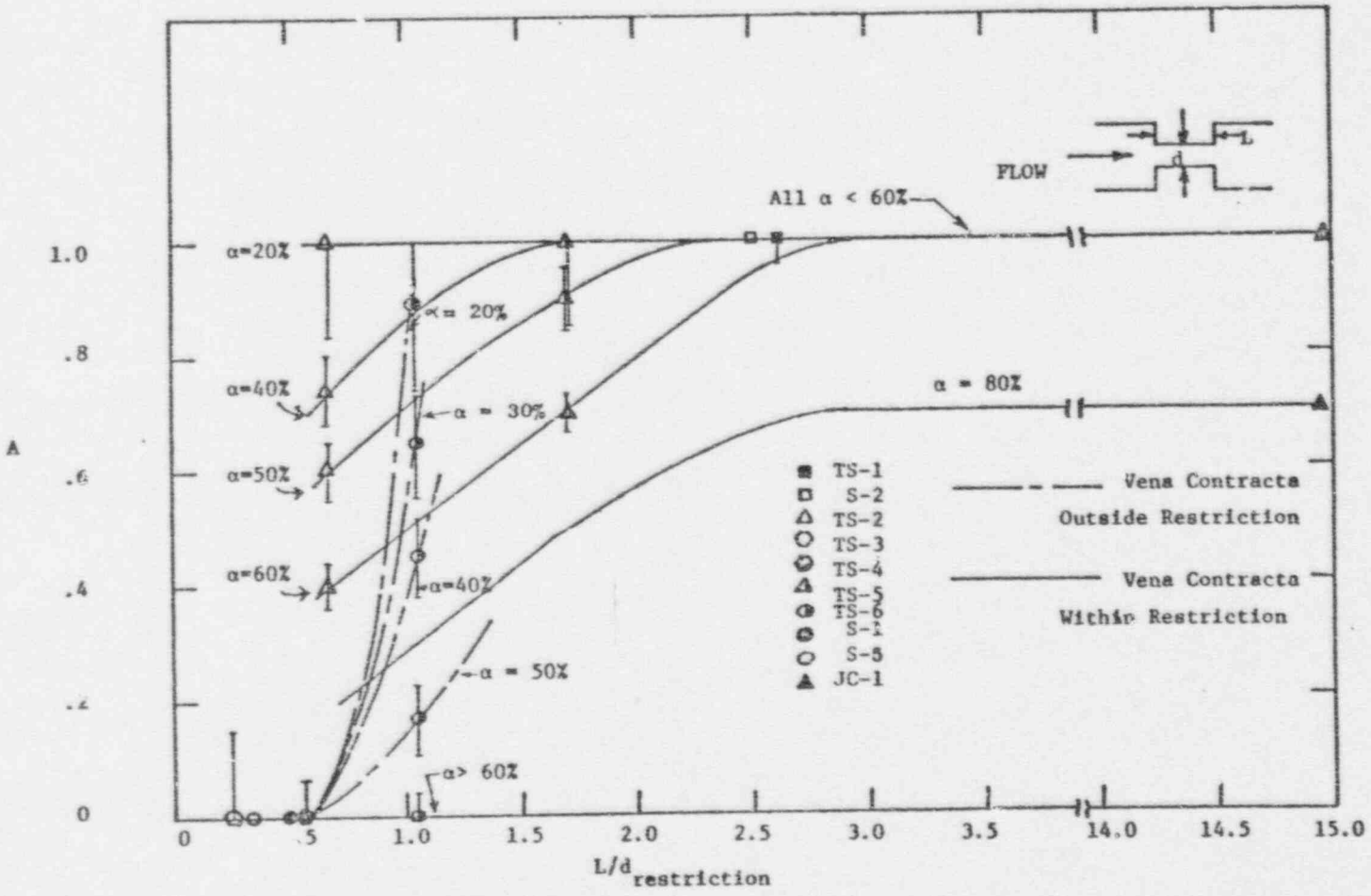

TABLE 5

JANSSEN[3] TEST SECTIONS

SECTION NO.	GEOMETRY	L_o INCHES	B_o	AREA RATIO σ
S-1	RECT.	.1	.2	.4
S-2	RECT.	.5	.2	.4
S-5	RECT.	.1	.3	.6
JC-1	CIRC.	10.0	.669	.492

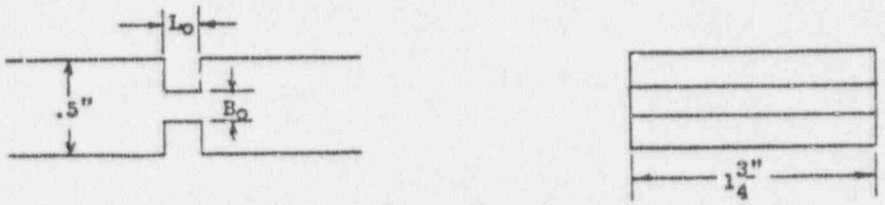

Rectangular Geometry

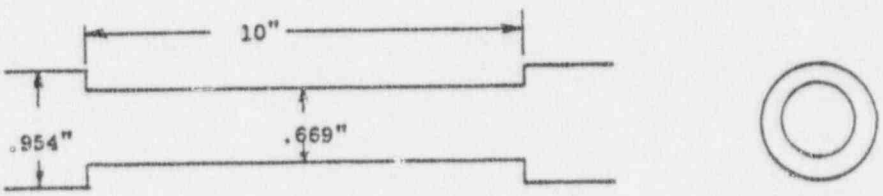

Circular Geometry

flow everywhere. The data of Fig. 18 indicate that when $(\frac{L}{d}$ restriction$)$ is below 0.5, A = 0 and hence slip flow should be assumed at all locations.

5.4 Application of Computational Procedures to Conditions With Substantial Vaporization

When a large difference is found between the inlet and outlet void fraction, a method for predicting the pressure loss is needed. Large differences between in the inlet and outlet void fractions were encountered with test section 6 when a flow of 4.6×10^6 lbm/hr ft^2 was used. Under conditions of nearly constant α, the pressure loss was predicted by the short insert equation (Eq. 12) because the vena contracta occured outside the restriction. To use (Eq. 11) a value for α at the vena contracta is required. When a large amount of vaporization occurs, the quality (x) at location 3 (vena contracta) may not be the same quality as at location 5. Several assumptions are possible. One may assume that α_3 should be based on the inlet quality, exit quality, or a quality midway between the two. The pressure drops computed with these assumptions were compared to the data. The mixing factor, A, for the vena contracta void fraction was evaluated using the void fraction consistent with the quality assumed at the vena contracta.

It was found that the pressure loss is best predicted by computing α_3 with the assumption that the quality at the vena contracta is the same as the outlet quality. (See Table 6). In using Eq.(12) for predicting the the pressure drop, the value of x was taken as the average of the vena contracta and exit qualities. The difference between this predicted value and the experimental value averages less than 5%. A sample calculation is given in Appendix I.

TABLE 6

PRESSURE LOSS PREDICTIONS

TEST NO.	C	PRESSURE LOSS			
		EXPERIMENTAL PSF	$X_{VC}=X_{INLET}$ PSF	$X_{VC}=X_{INLET}+X_{OUTLET}$ / 2 PSF	$X_{VC}=X_{OUTLET}$ PSF
TS-6-5-1	.71	395.8	no difference		
-2	"	491.5	403.0	441.8	480.1
-3	"	681.6	444.5	532.7	636.4
-4	"	773.7	485.6	627.8	774.8
-5	"	788.5	498.4	678.4	741.5
-6	"	648.7	433.5	526.1	610.5

6.0 Conclusions

The present investigation indicates that models based on a one dimensional momentum balance approach are adequate for the prediction of two-phase pressure losses across abrupt area changes for short, long, and intermediate length restrictions. The present work confirms Husain and Weisman's[1] previous conclusion that the two-phase pressure drop across well separated abrupt expansion-contraction combinations may be predicted by

$$\Delta p_{LOSS}\left(\begin{matrix}LONG\\INSERT\end{matrix}\right) = \frac{G_1^2}{2\rho_1 g_c}\left[\frac{1}{\sigma^2}\left(\frac{\rho_1}{\rho_g}x^2 a_1\left(\frac{1}{C^2 a_3^2} - \frac{1}{a_4^2}\right) + (1-x)^2(1-\hat{a}_1)\right.\right.$$

$$\left(\frac{1}{C^2(1-a_3)^2} - \frac{1}{(1-a_4)^2}\right)\Big\} - \frac{2}{\sigma^2}\left\{\frac{\rho_1}{\rho_g}x^2\left(\frac{1}{Ca_3} - \frac{1}{a_4} + \frac{\sigma}{\sigma_4} - \frac{\sigma^2}{a_5}\right)\right.$$

$$+ (1-x)^2\left(\frac{1}{C(1-a_3)} - \frac{1}{1-a_4} + \frac{\sigma}{1-a_4} - \frac{\sigma^2}{1-a_5}\right) + \frac{\rho_1}{\rho_g}x^2\hat{a}_2\left(\frac{1}{\sigma^2 a_4^2}\right. \qquad (20)$$

$$\left.\left.\left. - \frac{1}{a_1^2}\right) + (1-x)^2(1-\hat{a}_2)\left(\frac{1}{\sigma^2(1-a_4)^2} - \frac{1}{(1-a_1)^2}\right)\right\}\right]$$

where slip flow is assumed everywhere except at the vena contracta. At the vena contracta the flow is taken as homogeneous up to a void fraction of 50%. At higher void fractions mixing is incomplete and the void fraction is obtained from

$$a_3 = a_{slip} + A(a_{homog} - a_{slip}) \qquad (21)$$

where $A = 1.5 - a_4$,

From the present work, it is found that if the ratio $L/d_{restriction}$ is less than 2.0, the pressure drop may be predicted from the foregoing equation providing the vena contracta occurs within the restriction and

it is assumed that

a) the void fraction upstream of the expansion is the same as at the vena contracta.

b) the void fraction at the vena contracta is obtained from Equation 21 with the mixing factor, A, obtained from the solid lines in Figure 18.

This study has also confirmed the conclusion of Hoopes[16] and Janssen[2] that very short inserts behave differently from long inserts. When the vena contracta occurs outside the restriction, the pressure loss is given by

$$\Delta p_L\left(\begin{matrix}\text{SHORT}\\ \text{INSERT}\end{matrix}\right) = \frac{G_1 v_1}{2g_c\sigma^2}\frac{1}{C^2}\left[\frac{v_g}{v_1}x^2\hat{\alpha}_3\left(\frac{1}{\alpha_3}-\frac{\sigma^2C^2}{\alpha_5^2}\right)\right.$$

$$+(1-x)^2(1-\hat{\alpha}_3)\left\{\frac{1}{(1-\alpha_3)^2}-\frac{\sigma^2C^2}{(1-\alpha_5)^2}\right\}$$

$$\left.-2\sigma C\left[\frac{v_g}{v_1}x^2\left(\frac{1}{\alpha_3}-\frac{\sigma C}{\alpha_5}\right)+(1-x)^2\left(\frac{1}{1-\alpha_3}-\frac{\sigma C}{1-\alpha_5}\right)\right\}\right] \qquad (22)$$

If $(L/d_{\text{restriction}} \leq .5)$, Equation (22) may be used with the assumption of slip flow at all locations. The Hughmark[8] correlation is recommended to obtain the relationship between α and x.

When $(L/d_{\text{restriction}} > .5)$, the pressure loss can be predicted by the foregoing equation for short inserts providing the void fraction at the vena contracta is based on partial mixing at the vena contracta. The vena contracta void fraction may also be calculated from Equation (21) with the mixing factor obtained from the dashed lines of Figure 18.

The above approach is valid for both single hole and multiple hole restrictions. When multiple hole restriction are considered, the $(L/d_{\text{restriction}})$ ratio should be determined using the diameter of a

single hole.

When there is significant vaporization across the restriction, it is suggested that α_3 be based on the exit quality. (see section 5.4) It should be noted that use of either equation (19) or (21) implies that the quality variation across the insert is not large and that an average value of x (based on vena contracta and exit values) may be used.

The data considered in arriving at these conclusions included both steam-water and freon-freon vapor systems over a variety of pressures and void fractions. However, the mass flow rates used were in all cases at or above [illegible] lbs/hr ft^2 in the small size pipe or restriction. Caution should therefore be used in extrapolating these results to very low flow rates.

REFERENCES

(1) Husain, A. and Weisman, J., "Two Phase Pressure Drop Across Abrupt Area Changes", University of Cincinnati Report COO 2152-15 for the Nuclear Regulatory Commission (1975).

(2) Janssen, E., "Two Phase Pressure Loss Across Abrupt Contractions and Expansions, Steam-Water at 600 to 1400 PSIA," International Heat Transfer Conference, Chicago, 1966, ASME, Vol, 5, pg. 13-23.

(3) Lottes, P. A., "Expansion Losses In Two Phase Flow," Nuclear Science and Engineering, Vol. 9, 26-31, 1961.

(4) Mendler, O., "Sudden Expansion Losses in Single and Two Phase Flow," Ph.D. Dissertation, U. of Pittsburgh (1963).

(5) Ferrel, J. K. and J. W. McGee, U.S. AEC Report, "Two Phase Flow Through Abrupt Expansions and Contractions," TID-2339-Vol. 3(1966).

(6) Janssen, E. and Kervinen, J. A., "Two Phase Pressure Drop Across Expansions and Contractions; Water-Steam Mixtures at 600-1400 PSIA," General Electric Co. Report GEAP-4622 (1964)

(7) Fitzsimmons, D. E., "Two Phase Pressure Drop in Piping Components," Hanford Laboratory Report HW-80970 Rev. 1 (1964).

(8) Hughmark, G. A., Chem. Eng. Progress 58, (4), 62(1962).

(9) Husain, A., W. G. Choe and J. Weisman, "The Applicability and the Homogeneous Flow Model to Pressure Drop in Straight Pipe and Across Area Changes", University of Cincinnati Report COO-2152-16 (1975).

(10) Dukler, A. E., M. Wicks and R. G. Cleveland A.I.Ch.E. Journal 10, 44 (1964).

(11) Geiger, G. E., "Sudden Contraction Losses in Single and Two Phase Flow," Ph.D. Dissertation, U. of Pittsburgh (1964).

(12) James, R. "Metering of Steam-water Two Phase Flow by Sharp Edged Orifices" Proc. Inst. Mech Engrs 180, Pt 23, p 268 (1965-66)

(13) Murdock, J.W. "Two-Phase Measurement With Orifices", J. Basic Engineering 84, (4), 419 (1962).

(14) Collier, J. G. "Convective Boiling and Condensation" McGraw Hill Book Co., New York (1972).

(15) Chisholm D. and Leishman, J. "The Metering of Wet Steam" Chem & Proc. Eng. p 103 (July 1969).

(16) Hoopes, J. W. Jr., "Flow of Steam-Water Mixtures in a Heated Annulus and Through Orifices," A.I.Ch.E. Journal, June 1957, pages 268-75.

(17) Cermak, J. O., J. J. Jicha, and R. G. Lightner, Trans ASME, J. Heat Transfer, 86, 227 (1964).

(18) El Wakil, M. W., "Nuclear Power Engineering," pg. 288, McGraw Hill, New York (1962).

(19) Baroczy, C. J., "A Systematic Correlation for Two-Phase Pressure Drop," North American Report, NAA-SR-Memo-11858.

(20) Fluid Meters - Their Theory and Application Report of ASME Research Committee on Fluid Meters, Fifth Edition 1959, Published by The American Society of Mechanical Engineers, 29 West Thirty Nineth St., N.Y.

(21) Kays, W., and London. A. L., "Compact Heat Exchangers," p. 94, McGraw Hill, New York (1955).

Nomenclature

Fr - Froude No.

G - Mass flow rate (lbm/hr ft^2)

v - specific volume (ft^3/lbm)

σ - area ratio

g_c - gravitional constant

x - quality ($\frac{\text{lbm VAPOR}}{\text{lbm MIXTURE}}$)

α - void fraction ($\frac{\text{vol. of vapor}}{\text{vol. of mixture}}$)

C - vena contracta area ratio ($\frac{\text{area of vena contracta}}{\text{area of restriction}}$)

ρ - specific density (lbm/ft^3)

A - mixing factor

K - flow parameter related to slip (Hughmark's Correlation)

$\hat{\alpha}$ - average void fraction ($\frac{\text{vol. of vapor}}{\text{vol of mixture}}$)

Δp - pressure change (PSI)

Re - Reynolds No.

Subscripts

l - liquid

g - gas

e - expansion

c - contraction

x - x direction

L - loss

VC - vena contracta

a - acceleration

APPENDIX A

Experimental Procedure and Single Phase Calibration

1. Experimental Procedure

At the start of each test series, the zero of the differential pressure cell was checked and then the pump was started. The desired flow rate was set and the system pressure was set with a pressure regulator. The heaters were then turned on and the system slowly heated. During this period, the Freon was all liquid and two checks were made. The single phase pressure drop and void sensor readings were observed to be a function of the temperature of the fluid. These were compared with previous observations at the same temperatures.

Once two-phase operation began, the heat input was increased in a stepwise manner. The system was allowed to stablize between the step increases in heat input. At that time both void sensors were read and checked for repeatability, and the differential pressure across the test section recorded. A constant flow rate was maintained by adjusting a pump bypass valve. Sufficient coolant flow was permitted to the condenser to provide a subcooled liquid to the pump and prevent cavitation.

Once the series of tests was complete, the single phase operation was resumed and the temperature dependency of the single phase pressure loss and the void sensors checked to be certain no changes in the instrumentation had occurred during the test.

2. Single Phase Calibration

Temperature was found to have a small effect on the single phase pressure drop. This is shown in Figures 19-24. This is due to the change in the Reynolds Number, which varies inversely with the viscosity. For Freon 113, the viscosity changes by over 10% with only a 20°F change in

fluid temperature. The increase in temperature decreases the viscosity which increases the Reynolds Number.

This observation was found to be consistent with the work of Kays [21] who found that single phase abrupt area change loss coeficients vary with the Reynolds Number. The contraction coefficient decreases with increasing Reynolds Number while the expansion coefficient increases with Reynolds Number, but at a slower rate than the contraction coefficient changes. Therefore, the combined loss coefficient would decrease with Reynolds Number, and so the observed pressure loss would decrease with increasing temperature.

It should be noted that the pressure loss discussed does not include the loss associated with frictional drag of the fluid on the pipe. The frictional loss in the pipe was accounted for by the use of the Baroczy [19] correlation.

The single phase pressure loss is seen to decrease in Figures A1-A6 with increasing temperature. A decrease was not observed in Figure 8 due to the large single phase pressure loss associated with that insert, (TS-6). Only a 3 or 4 PSF decrease was noted in the first five inserts which represented a pressure change of at least 3 or 4 %, which could be detected by the instrumentation. The single phase pressure loss was very large for the sixth test section and the instrumentation may not have been detect these small changes in a pressure drop this large. The pressure loss thus appeared to be essentially constant over the temperature range investigated.

The single-phase pressure drop data were also used to obtain the value of C, the vena contracta area ratio; for each of the test sections. Where the vena contracta was inside the insert, the value of C was obtained from

$$\Delta p_L \left(\begin{matrix}\text{Long}\\ \text{Insert}\end{matrix}\right)_{1\phi} = \frac{G_1^2}{2g_c\rho_1\sigma^2}\left[1-2\sigma+\sigma^2+\frac{1}{C^2}-\frac{2}{C}+1\right] \qquad (A\text{-}1)$$

When the vena contracta was estimated to be outside the test section, C was obtained from

$$\Delta p_L \left(\begin{matrix}\text{SHORT}\\ \text{INSERT}\end{matrix}\right)_{1\phi} = \frac{G_1^2}{2g_c\sigma^2\rho_1}\frac{1}{C^2}\left[1-2\sigma C+\sigma^2C^2\right] \qquad (A\text{-}2)$$

The values of C obtained for a temperature of 190°F are tabulated in table A-1. It is seen that in all cases the values of C obtained lie within the range expected. It will also be observed that the value of C tends to increase with increasing G. This implies a lower pressure drop at higher G's or higher Reynolds number. This is in agreement with the previously noted temperature effect.

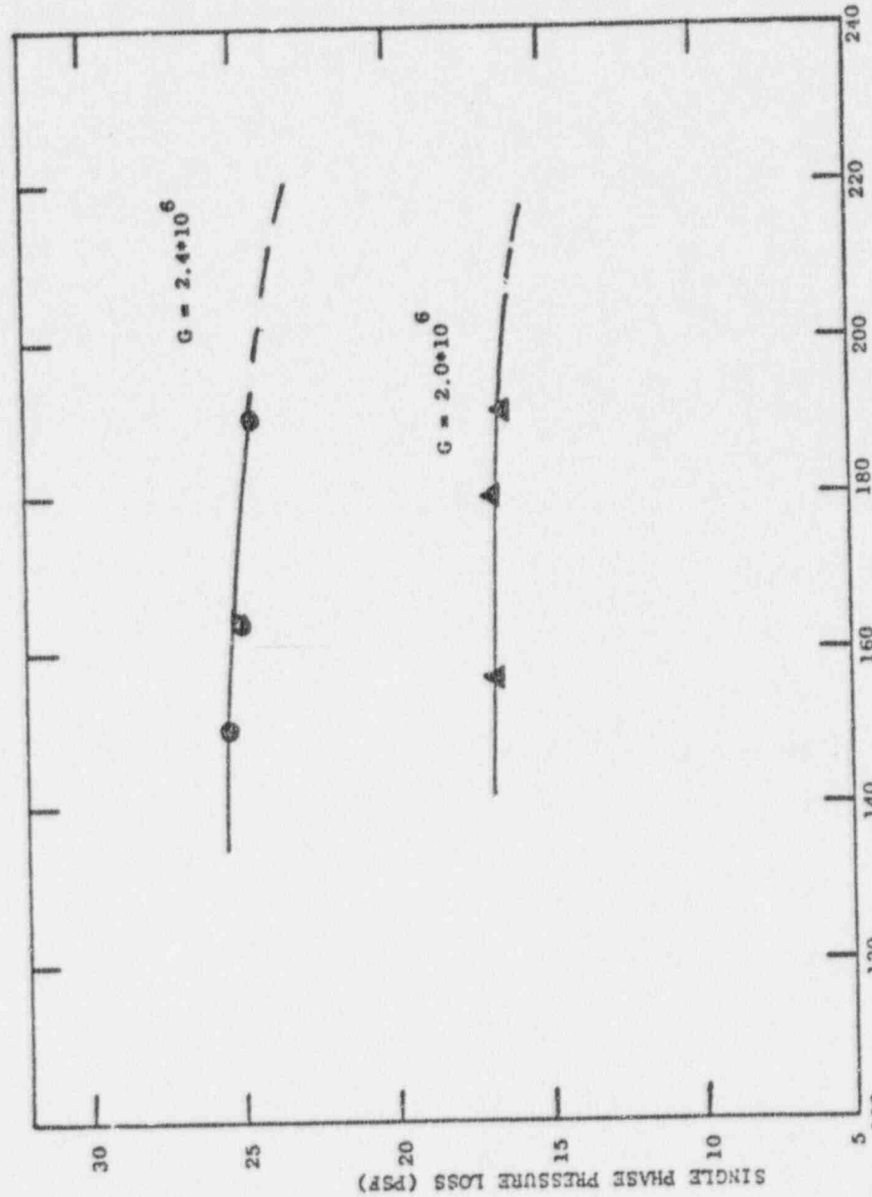

FIG.A1 SINGLE PHASE PRESSURE DROP vs FLUID TEMPERATURE for TS-1

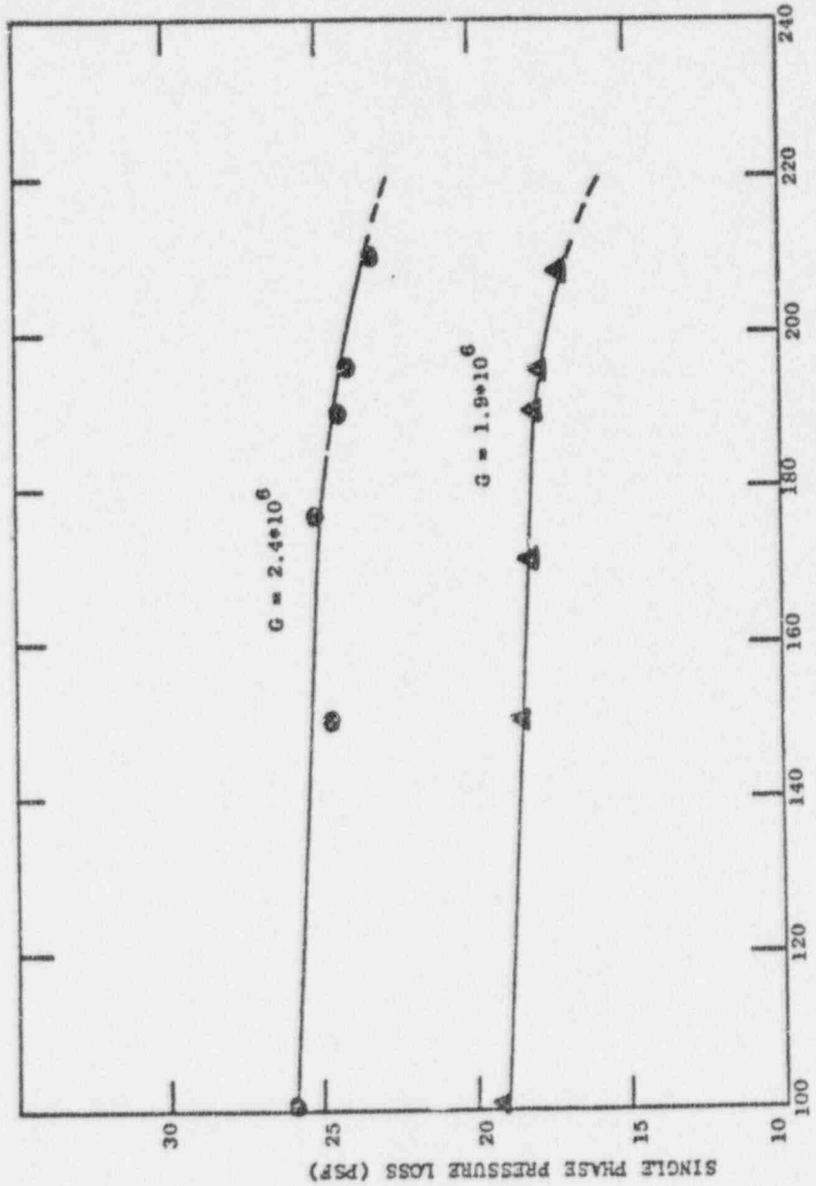

FIG. A2 SINGLE PHASE PRESSURE DROP vs FLUID TEMPERATURE for TS-2

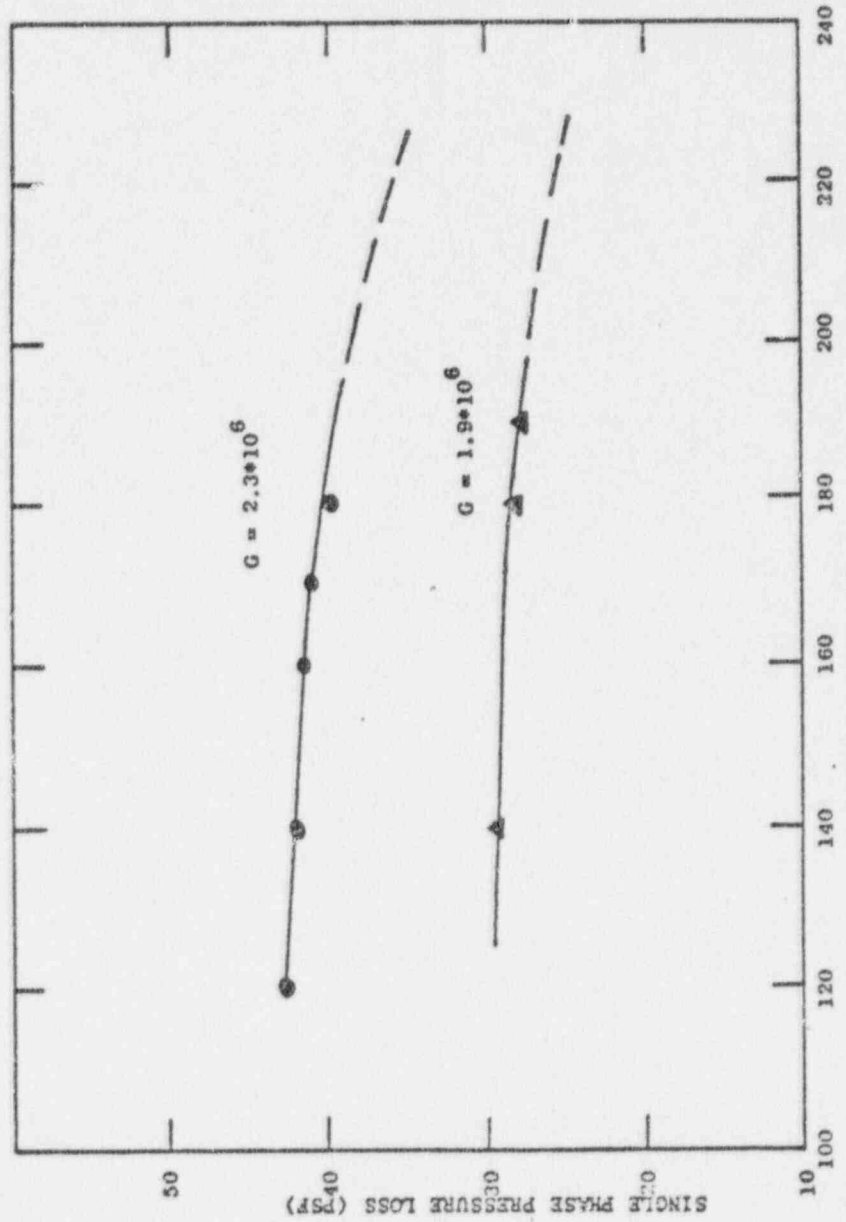

FIG.A3 SINGLE PHASE PRESSURE DROP vs FLUID TEMPERATURE for TS-3

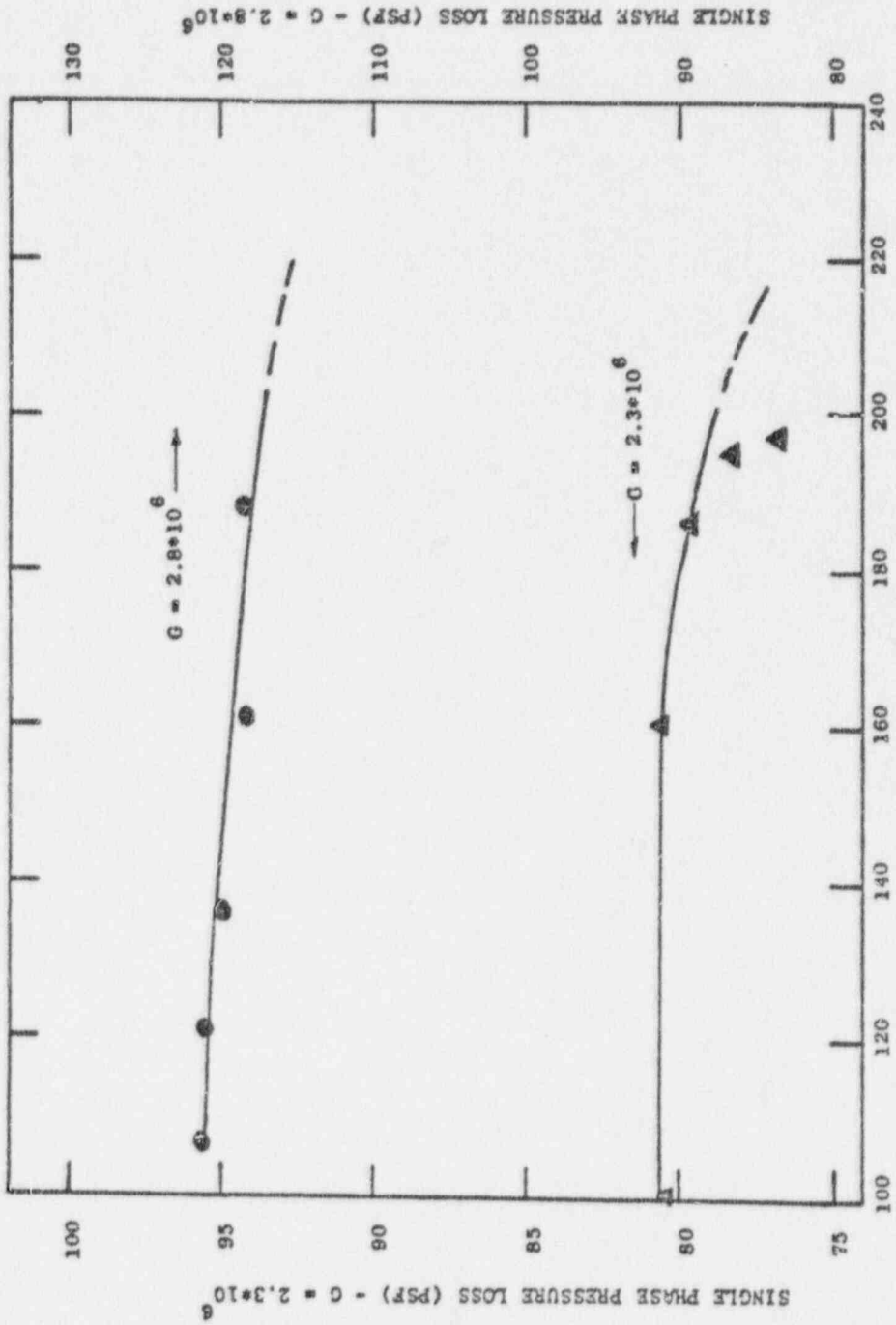

FIG.A4 SINGLE PHASE PRESSURE DROP vs FLUID TEMPERATURE for TS-4

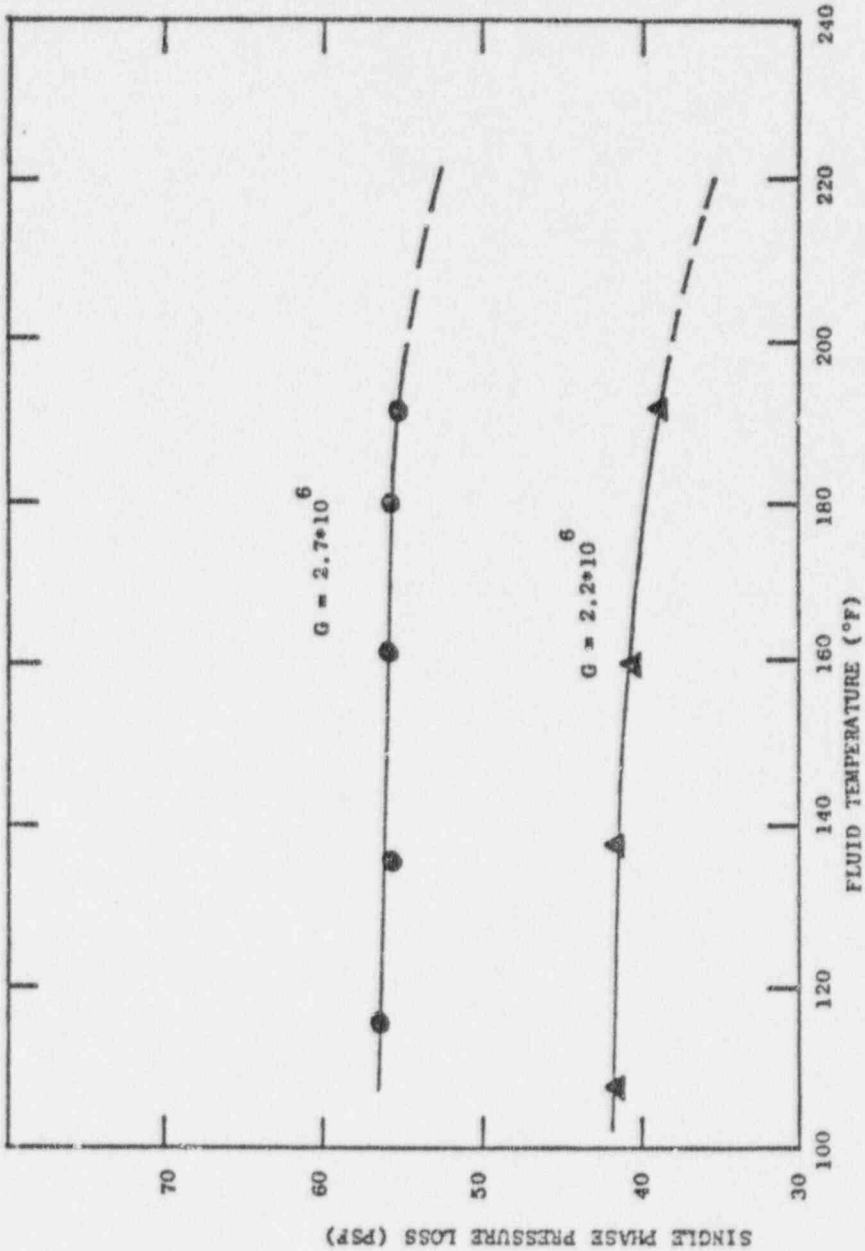

FIG. A5 SINGLE PHASE PRESSURE DROP vs FLUID TEMPERATURE for TS-5

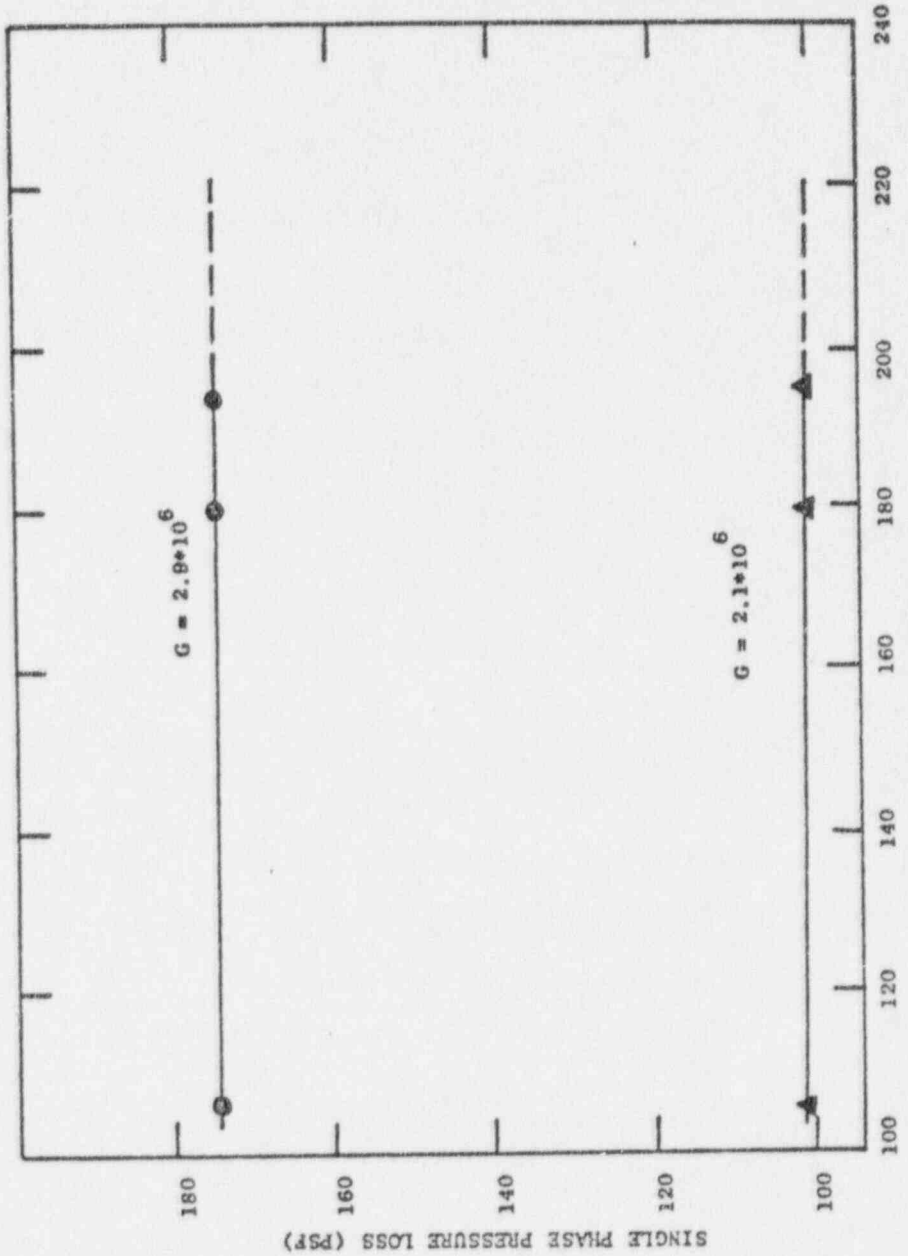

FIG.A6 SINGLE PHASE PRESSURE DROP vs FLUID TEMPERATURE for TS-6

TABLE A-1

VENA CONTRACTA AREA RATIO

TEST SECTION	FLOW	VENA CONTRACTA AREA RATIO	FLOW AREA RATIO	HDMT EQ. USED
	$lb/HR\text{-}FT^2$	C	σ	
TS-1	2.0×10^6	.711	.590	LONG INSERT
	2.4-2.8	.714		Eq(A-1)
TS-2	1.9×10^6	.687	.595	LONG INSERT
	2.4×10^6	.721		Eq(A-1)
TS-3	1.9×10^6	.718	.615	SHORT INSERT
	2.3-2.7	.732		Eq(A-2)
TS-4	2.3×10^6	.638	.505	SHORT INSERT
	2.8×10^6	.643		Eq(A-2)
TS-5	2.2×10^6	.610	.534	LONG INSERT
	2.7×10^6	.624		Eq(A-1)
TS-6	2.1×10^6	.624	.249	SHORT INSERT
	2.9×10^6	.662		Eq(A-2)

APPENDIX B

Reduction Procedure

The data reduction scheme used will be illustrated by Run No. TS-3-6-1

(1) Calculation of Mass Flow

This measurement was taken using an orifice plate which was installed between the pump and the immersion heaters. The flow was calculated from the equation

$$W = CA_2\sqrt{2g_c \Delta p \rho}_L \quad (\text{lbm/sec})$$

Since the Δp was measured in units of inches of water, then

$$\Delta p = \rho_w H_w g/g_c$$

where H_w is the difference between the two water columns in the manometer

ρ_w is the density of water (lbm/ft^3)

A_c for the orifice used was equal to .0064

C was supplied by the manufacturer for the range of operation and was equal to .685. [Orifice and pipe assembly was constructed in accordance with ASME specifications. Value of C was checked by following procedures of ASME Fluid Meters handbook]

Upon insertion of the above constants and conversion factors, the mass flow rate equation becomes

$$W = .0801\sqrt{\rho_{FREON} * \Delta H_w}$$

For the present run:

$$\Delta H_w = 10\text{" of water (held constant)}$$

$$\rho_{FREON} = 92.33 \text{ lbm/ft}^3$$

$$W = .0801 \sqrt{92.33 * 10}$$

$$= 2.434 \text{ lbm/sec}$$

In the large pipe the diameter was .991 inches. In the restriction the diameter was .777 inches.

The mass flux in each pipe is given by

$$G = \frac{W}{A} \times 3600 \text{ (lbm/hr ft}^2\text{)}$$

where W is the mass flow (lb/sec) A is the cross sectional area of the pipe (ft^2)

For the large pipe

$$G_{LARGE} = \frac{2.434}{(\frac{.991}{2})^2/4} 3600$$

$$= 1.636 \times 10^6 \text{ lbm/hr ft}^2$$

For the small pipe

$$G_{SMALL} = \frac{2.434}{(\frac{.777}{12})^2/4} 3600$$

$$= 2.661 \times 10^6 \text{ lbm/hr ft}^2$$

Since $\Delta p_{i\phi} = (f \frac{L}{D} \frac{G^2}{2 g_c})_{LARGE} + (f \frac{L}{D} \frac{G}{2 g_c})_{SMALL}$

$$\text{or } \Delta P_{ST_{TP}} = \Delta P_1 \phi^2_{\text{LARGE}} \text{MULTIPLIER} + \Delta P_1 \phi^2_{\text{RESTRICTION}} \text{MULTIPLIER}$$

$$\Delta P_{ST_{TP}} = 10.30\ (2.001) + .318\ (1.679)$$

$$= 21.2 \text{ PSF}$$

then

$$\Delta P_{L + \text{ACCEL} + \text{NON-RECOVERY}} = 127.5 - 21.2 = 106.3 \text{ PSF}$$

(2) Estimation of Void Fraction

As previously noted, the void fraction was measured by using a capacitance type void sensor. The meter was calibrated to give 0 → 10 voltage difference when the void was ranged from 0 to 100%.

To correct for the variation of the zero void reading with temperature, temperature and voltage readings were taken with liquid Freon flowing through the sensor. The voltage reading was assumed to vary linearly with void between the zero and 100% void readings (see Appendix A for void meter calibration). With these assumptions, the void fraction was determined to be 44.8% for the run.

(3) Pressure Drop Across Abrupt Expansion and Contraction

3a Differential cell reading = 81.7%. Since full scale corresponded to 30" of water differential, then

$$\Delta p_{L + f + \text{ACCEL.} + \text{NON-RECOVERY}} = .81.7 \times 30 = 24.51 \text{ inches of water}$$

$$= 127.5 \text{ PSF}$$

3b Estimation of Straight Pipe Friction Loss

Large Pipe: 18" length, .991" diameter

Restriction: .215" length, .777" diameter

Using the Baroczy Correlation

$$\Delta p_{ST_{TP}} = \Delta p_{ST_{TP}} \text{ (large pipe)} + \Delta p_{ST_{TP}} \text{ (restriction)}$$

(4) Correction for Vaporization

Void fraction measurements indicate no significant vaporization across the test section at low mass velocities. Therefore no flashing correction was made to the preceding sample run. At the highest mass velocity's flashing gives rise to an acceleration term which should be subtracted from the measured data

(5) Calculation of Acceleration Pressure Drop

The acceleration pressure drop is given by

$$\Delta p_a = r \frac{G^2}{g_c}$$

where G is the mass flux from part (1)

g_c is $4.17 \times 10^8 \frac{\text{lbm ft}}{\text{lbf hr}^2}$

r is an acceleration multiplier given by

$$r = v_f \left[\frac{(1-x_e)^2}{1-\alpha_e} + \frac{x_e^2}{\alpha_e} \frac{v_g}{v_f} - 1 \right]$$

where v_f is the specific volume of the liquid

v_g is the specific volume of the gas

x_e is the exit quality

α_e is the exit void fraction

Since the inlet is a vapor instead of a saturated liquid, an r is calculated for the inlet and one for the outlet. The difference is then multiplied by $\frac{G^2}{g_c}$

For this run

$$\alpha_{inlet} = 43.6\% \quad \alpha_{outlet} = 46.0\%$$

$$x_{inlet} = 2.47\% \quad x_{outlet} = 2.76\%$$

$$v_g = .5556 \text{ ft}^3/\text{lbm} \quad v_f = .0116^{\text{c}} \text{ ft}^3/\text{lbm}$$

substituting, it is found

$$r_{inlet} = .0088 \quad r_{outlet} = .0097$$

so

$$\Delta P_{ACCEL} = (.0097-.0088) \frac{(1.636\times10^6)^2}{4.17\times10^8}$$

$$= 5.7\text{PSF}$$

then

$$\Delta P_{L+NON-RECOVER} = 106.3-5.7 = 100.6 \text{ PSF}$$

(6) Correction for Undeveloped Expansion Pressure Loss

The loss due to undeveloped pressure recovery for various distances after an expansion was investigated by Mendler[6] and Janssen and Kervinen[8], and is extensively discussed in Appendix E and F. The curve for correcting for non-recovery is shown in Figure 9. For $\alpha = 44.8$,

$$\frac{\Delta P_{FULLY\ RECOVERED}}{\Delta p \text{ at } L/D = 12} = .96$$

$$\Delta P_{FULLY\ RECOVERED} = .96*100.6$$

$$= 96.58 \text{PSF}$$

then the excess rise is

$$\Delta P_{NON-RECOVER} = 100.6-96.6 = 4.0 \text{PSF}$$

finally

$$\Delta P_L = 100.6-4.0 = 96.6 \text{ PSF}$$

APPENDIX C

Data Tabulation

Nomenclature

σ - area ratio $\left(\frac{\text{restriction flow area}}{\text{pipe flow area}}\right)$

P - System pressure (PSIG)

G - Restriction Mass Flow Rate (lb/hr ft^2)

Measured pressure loss - Pressure drop as recorded from differential pressure cell (PSF)

Friction loss - Pressure loss between the pressure taps due to the drag of the liquid on the pipe and restriction walls (PSF)

Accel. loss - Pressure loss due to vaporization of liquid across the the restriction (PSF)

Non-Rec loss - Excessive pressure loss due to measuring the pressure before the pressure had fully recovered from an expansion (PSF)

Corr. pressure - Measured loss minus the sum of the friction, acceleration, and non-recovery losses (PSF)

Single Phase loss - Pressure loss across the restriction at the test temperature if the fluid was entirely liquid at the test conditions (PSF)

Pres. Ratio - (Corrected pressure)/(Single phase pressure)

TS-1 σ = .590

P = 25PSIG

G = 2.0×10^6

RUN NUMBER	VOID FRACTION	MEASURED PRESSURE LOSS	FRICTION LOSS	ACCEL LOSS	NON-REC LOSS	CORR. PRES	SINGLE PHASE PRESS	PRES. RATIO
TS-1-1-1	34.2	59.3	16.5			42.8	16.3	2.63
-2	31.9	57.7	15.7			42.0	16.3	2.58
-3	2.1	26.5	8.5			18.0	16.6	1.09
-4	5.9	26.5	8.5			18.0	16.5	1.09
-5	41.1	68.7	20.5		.5	47.7	16.3	2.93
-6	43.1	71.8	21.8		1.3	48.8	16.3	3.00
-7	47.9	87.4	25.0		3.7	58.7	16.3	3.61

P = 25 PSIG G = 2.4×10^6

TS-1-2-1	25.9	65.6	18.5			47.1	24.9	1.89
-2	36.8	90.5	24.0			66.5	24.8	2.68
-3	17.1	49.9	15.5			34.4	25.0	1.37
-4	12.9	43.7	14.5			29.2	25.1	1.16
-5	4.1	40.6	12.6			28.0	25.3	1.11

RUN NUMBER	VOID FRACTION	MEASURED PRESSURE LOSS	FRICTION LOSS	ACCEL LOSS	NON-REC LOSS	CORR. PRES	SINGLE PHASE PRESS	PRES. RATIO
			P = 25 PSIG G = 2.8×10^6					
TS-1-3-1	9.2	57.7	15.1			42.6	36.8	1.16
			P = 40 PSIG G = 2.0×10^6					
TS-1-4-1	33.7	56.2	14.7			41.5	16.4	2.53
-2	44.5	68.7	19.2		1.7	47.7	16.4	2.91
-3	39.7	62.4	17.0			45.4	16.3	2.78
-4	25.9	49.9	12.0			37.9	16.6	2.29
-5	21.0	43.7	10.8			32.9	16.6	1.98
-6	6.0	25.0	8.1			16.9	16.9	1.00
-7	11.1	30.0	8.8			20.9	16.8	1.25
-8	20.4	42.1	10.5			31.6	16.6	1.91
-9	12.3	31.2	8.8			22.4	16.8	1.34
			P = 40 PSIG G = 2.4×10^6					
TS-1-5-1	15.1	49.9	14.2			35.7	24.4	1.46
-2	20.1	55.6	15.9			39.7	24.4	1.63
-3	35.5	81.2	21.2			60.0	24.3	2.47
-4	25.5	61.8	17.5			44.3	24.3	1.82
-5	42.0	96.8	24.5		1.1	71.2	24.3	2.94
-6	54.3	143.6	33.5		12.1	98.0	24.2	4.05

P = 40 PSIG G = 2.8×10^6

RUN NUMBER	VOID FRACTION	MEASURED PRESSURE LOSS	FRICTION LOSS	ACCEL LOSS	NON-REC LOSS	CORR. PRES	SINGLE PHASE PRESS	PRES. RATIO
TS-1-6-1	31.1	98.3	21.3			77	36.1	2.13

P = 60 PSIG G = 2.4×10^6

TS-1-7-1	2.8	38.1	11.7			26.4	23.7	1.11
-2	6.2	40.6	11.9			28.7	23.7	1.21
-3	14.0	47.8	13.1			34.7	23.6	1.47
-4	56.1	138.9	34.0		12.6	92.3	23.4	3.95
-5	54.8	132.7	32.5		11.5	88.7	23.4	3.80
-6	14.4	49.9	13.2			36.7	23.57	1.56
-7	32.2	73.3	18.0			55.3	23.5	2.36
-8	48.7	113.9	27.2		6.1	80.6	23.4	3.45

TS-2 σ = .595

P = 40 PSIG G = 1.9×10^6

TS-2-1-1	27.2	42.9	10.3			32.6	18.0	1.81
-2	35.9	46.8	12.3			34.5	18.0	1.92
-3	31.1	45.3	10.3			35.0	18.0	1.94
-4	18.7	43.7	8.2			35.5	18.2	1.95
-5	30.7	46.0	11.3			34.7	18.1	1.92
-6	23.2	42.9	9.2			33.7	18.1	1.86
-7	33.2	49.2	11.8			37.4	18.1	2.07
-8	40.8	56.2	14.5		.4	41.3	18.0	2.29

TS-2 = .595

P = 40 PSIG G = 1.9×10^6

RUN NUMBER	VOID FRACTION	MEASURED PRESSURE LOSS	FRICTION LOSS	ACCEL LOSS	NON-REC LOSS	CORR. PRES	SINGLE PHASE PRESS	PRES. RATIO
TS-2-1-9	57.1	85.8	23.0		8.2	54.6	17.9	3.05
-10	52.8	79.6	20.2		5.9	53.5	18.0	2.98
-11	50.4	73.3	19.0		4.3	50.0	18.0	2.78
-12	44.8	64.8	15.3		2.0	47.5	18.0	2.64
-13	51.5	79.6	19.8		5.4	54.4	18.0	3.03
-14	55.5	84.3	22.5		7.1	54.7	18.0	3.05
-15	54.4	82.7	21.8		6.7	54.2	18.0	3.02
-16	59.3	92.1	25.5		9.7	56.9	17.9	3.18
-17	59.9	95.2	26.5		10.3	58.4	17.9	3.26

P = 40 PSIG G = 2.4×10^6

TS-2-2-1	24.2	54.6	12.7			41.9	24.3	1.72
-2	27.8	58.5	14.0			44.5	24.2	1.84
-3	30.8	64.0	16.0			48.0	24.2	1.99
-4	33.3	67.9	15.0			51.9	24.1	2.15
-5	35.0	70.2	17.0			53.2	24.1	2.21
-6	42.2	82.7	20.0		.9	61.8	24.0	2.57
-7	1.1	33.6	9.5			24.1	25.1	.96
-8	48.9	101.4	25.0		5.3	71.1	24.0	2.96
-9	56.9	132.7	31.8		13.1	87.8	24.0	3.67

P = 60 PSIG G = 1.9×10^6

RUN NUMBER	VOID FRACTION	MEASURED PRESSURE LOSS	FRICTION LOSS	ACCEL LOSS	NON-REC LOSS	CORR. PRES	SINGLE PHASE PRESS	PRESS. RATIO
TS-2-3-1	4.4	25.0	6.3			18.7	16.2	1.16
-2	5.95	25.8	6.5			19.3	16.1	1.20
-3	8.0	26.5	6.7			19.8	16.1	1.23
-4	19.5	35.9	8.0			27.9	16.0	1.75
-5	26.8	44.5	9.3			35.2	15.9	2.22
-6	35.3	45.3	11.3			34.0	15.9	2.14
-7	40.3	47.6	12.8			34.8	15.8	2.20
-8	44.8	55.4	14.5		1.6	39.3	15.8	2.49
-9	50.1	61.6	17.0		3.3	41.3	15.7	2.62
-10	54.6	65.6	19.3		5.1	41.2	15.7	2.62

P = 60 PSIG G = 2.4×10^6

TS-2-4-1	44.4	79.6	20.2		2.1	57.3	22.8	2.51
-2	45.0	80.4	20.8		2.4	57.2	22.8	2.51
-3	48.8	84.3	23.0		4.3	57.0	22.8	2.50
-4	54.3	99.9	26.5		8.1	65.3	22.8	2.87
-5	30.6	58.5	14.9			43.6	22.9	1.90
-6	33.3	59.3	15.9			43.4	22.9	1.90
-7	35.3	62.4	16.5			45.9	22.9	2.01
-8	40.8	70.2	19.0		.5	50.7	22.8	2.22
-9	32.3	58.5	15.7			42.8	22.9	1.87
-10	24.1	47.6	13.3			34.3	22.9	1.50

P = 60 PSIG G = 2.4×10^6

RUN NUMBER	VOID FRACTION	MEASURED PRESSURE LOSS	FRICTION LOSS	ACCEL LOSS	NON-REC LOSS	CORR. PRES	SINGLE PHASE PRESS	PRES. RATIO
TS-2-4-11	24.5	49.2	13.5			35.7	22.9	1.56
-12	14.4	38.2	11.2			27.0	23.0	1.17
-13	11.8	36.7	10.9			25.8	23.0	1.12

TS-3 σ = .615

P = 25 PSIG G = 1.9×10^6

TS-3-1-1	5.4	36.9	6.3			30.6	29.3	1.04
-2	11.9	40.8	7.2			33.6	29.1	1.15
-3	26.2	54.1	10.5			43.6	29.1	1.50
-4	31.2	58.8	12.0			46.8	29.0	1.61
-5	34.3	63.5	13.0			50.5	29.0	1.74
-6	29.4	59.6	11.4			48.2	29.0	1.66
-7	41.4	66.6	16.0		.5	50.1	28.7	1.75

P = 40 PSIG G = 1.9×10^6

TS-3-2-1	4.3	36.2	6.3			29.9	28.3	1.06
-2	6.1	36.2	6.3			29.9	28.3	1.06
-3	18.8	43.2	8.3			34.9	28.0	1.25
-4	39.5	63.5	13.5			50.0	27.8	1.80
-5	41.3	65.8	14.3		.5	51.0	27.8	1.83
-6	46.1	74.4	16.2		2.9	55.3	27.7	2.00
-7	46.6	74.4	16.4		2.9	55.1	27.7	1.99
-8	47.7	75.2	17.0		3.2	55.0	27.7	1.99
-9	53.7	82.2	19.5		6.3	56.4	27.7	2.04

40 PSIG G = 2.3×10^6

RUN NUMBER	VOID FRACTION	MEASURED PRESSURE	FRICTION LOSS	ACCEL LOSS	NON-REC LOSS	CORR. PRES	SINGLE PHASE PRESS	PRES. RATIO
TS-3-3-1	1.8	51.8	8.5			43.3	40.5	1.07
-2	1.2	51.8	8.5			43.3	40.3	1.07
-3	2.6	51.8	8.5			43.3	40.3	1.07
-4	4.2	53.3	8.7			44.6	40.0	1.12
-5	6.5	53.3	9.0			44.3	40.0	1.11
-6	4.5	52.5	8.8			43.7	40.5	1.08
-7	8.3	54.9	9.2			45.7	40.0	1.14
-8	12.7	58.0	9.7			48.3	40.0	1.21
-9	19.3	62.7	11.2			51.5	39.8	1.29
-10	29.7	76.0	13.7			62.3	39.5	1.58
-11	32.1	79.1	14.5			64.6	39.5	1.64
-12	36.4	85.3	16.3			69.0	39.5	1.75
			60 PSIG G = 1.9×10^6					
TS-3-4-1	.9	35.4	5.8			29.6	27.3	1.08
-2	1.9	34.6	5.9			28.7	26.8	1.07
-3	9.0	38.5	6.5			32.0	26.4	1.21
-4	23.9	47.9	8.5			39.4	26.2	1.50
-5	22.0	46.3	8.1			38.2	26.0	1.47
-6	37.3	58.8	11.3			47.5	26.0	1.83
-7	34.5	58.0	10.6			47.4	26.0	1.82
-8	43.9	68.1	13.3		1.6	53.2	25.9	2.05

P = 60 PSIG G = 2.3×10^6

RUN NUMBER	VOID FRACTION	MEASURED PRESSURE	FRICTION LOSS	ACCEL LOSS	NON-REC LOSS	CORR. PRES	SINGLE PHASE PRESS	PRES. RATIO
TS-3-5-1	3.2	52.5	8.5			44.0	37.8	1.16
-2	6.3	54.1	8.5			45.6	37.8	1.21
-3	12.5	57.2	9.0			48.2	37.1	1.30
-4	29.3	70.5	12.4			58.1	36.6	1.59
-5	37.7	82.2	14.8			67.4	36.5	1.85
-6	37.4	78.3	14.7			63.6	36.5	1.74
-7	46.9	99.4	19.0		4.0	76.4	36.2	2.11
-8	53.7	110.3	22.9		8.7	78.7	36.0	2.19

P = 60 PSIG G = 2.7×10^6

TS-3-6-1	44.8	127.4	21.2	5.7	4.0	96.6	56.1	1.72
-2	46.1	129.0	22.0	3.7	4.6	98.7	56.1	1.76
-3	25.3	90.0	14.9	2.2		73.8	56.4	1.31
-4	27.7	91.6	14.7	3.4		73.5	56.4	1.30
-5	27.0	91.6	14.5	1.7		75.4	56.4	1.34
-6	19.1	82.2	13.8	1.6		66.8	58.6	1.15
-7	4.6	70.5	10.5	.9		59.1	56.9	1.04
-8	3.5	69.7	10.5	.4		58.8	56.9	1.03
-9	2.1	68.9	10.4	0		58.5	57.1	1.02

TS-4 σ = .505

P = 25 PSIG G = 2.3×10^6

RUN NUMBER	VOID FRACTION	MEASURED PRESSURE	FRICTION LOSS	ACCEL LOSS	NON-REC LOSS	CORR. PRES	SINGLE PHASE PRESS	PRES. RATIO
TS-4-1-1	8.4	84.3	7.5			76.8	87.3	.88
-2	10.9	85.8	7.8			78.0	87.3	.89
-3	9.3	95.2	7.7			87.5	80.5	1.09
-4	18.5	109.2	9.2			100.0	80.5	1.24
-5	20.7	112.3	9.6			107.8	80.5	1.28
-6	26.3	128.0	11.0			117.0	80.5	1.45
-7	33.5	143.5	13.4			130.2	80.5	1.62
			P = 25 PSIG G = 2.8×10^6					
TS-4-2-1	19.4	149.8	13.0			136.8	119.5	1.14
-2	29.3	171.7	16.3			155.4	119.0	1.31
-3	38.1	202.9	20.3			182.6	119.0	1.53
-4	34.2	212.2	18.0			194.2	119.5	1.63
-5	22.9	177.9	14.0			163.9	119.3	1.37
-6	34.8	187.3	18.0			169.3	119.0	1.42
-7	37.0	202.9	19.3			183.6	119.0	1.54
-8	13.9	143.6	11.3			132.3	119.8	1.10

RUN NUMBER	VOID FRACTION	MEASURED PRESSURE	FRICTION LOSS	ACCEL LOSS	NON-REC LOSS	CORR. PRES	SINGLE PHASE PRESS	PRES. RATIO
			P = 40 PSIG G = 2.3×10^6					
TS-4-3-1	6.8	85.8	7.0			78.8	80.0	.99
-2	24.0	113.9	9.7			104.2	79.5	1.31
-3	48.9	168.5	18.0		10.5	140.0	78.8	1.78
-4	53.0	190.4	20.2		17.0	153.2	78.8	1.94
-5	50.1	193.5	18.5		13.1	161.9	78.8	2.05
-6	48.8	190.4	18.0		12.1	160.3	78.8	2.03
			P = 60 PSIG G = 2.3×10^6					
TS-4-4-1	2.3	92.1	6.3			85.8	77.2	1.11
-2	7.8	93.6	6.8			86.8	76.5	1.13
-3	10.2	96.8	7.2			89.6	76.3	1.17
-4	18.9	106.1	8.4			97.7	76.1	1.28
-5	19.7	106.1	8.5			97.6	76.1	1.28
-6	25.3	117.0	9.0			108.0	76.0	1.42
-7	31.6	126.4	10.5			115.9	75.5	1.54
-8	38.9	137.3	12.5			124.8	75.5	1.65
			P = 60 PSIG G = 2.8×10^6					
TS-4-5-1	16.9	149.8	11.0			138.8	118.5	1.17
-2	26.1	165.4	13.0			152.4	118.0	1.29
-3	40.0	199.8	16.5			183.3	117.7	1.56
-4	41.1	206.0	16.7		1.9	187.4	117.7	1.59
-5	11.4	140.5	9.8			130.7	118.5	1.10

TS-5 σ = .534

P = 25 PSIG G = 2.7×10^6

RUN NUMBER	VOID FRACTION	MEASURED PRESSURE	FRICTION LOSS	ACCEL LOSS	NON-REC LOSS	CORR. PRES	SINGLE PHASE PRESS	PRES. RATIO
TS-5-1-1	2.5	68.7	11.7			57.0	56.0	1.02
-2	6.4	76.3	11.9			64.6	55.8	1.16
-3	27.8	112.4	18.8	1.4		92.2	55.8	1.65
-4	42.4	171.7	27.6	5.0	3.5	135.6	55.5	2.46
-5	42.0	168.5	27.3	6.9	2.7	131.6	55.6	3.37
			P = 40 PSIG G = 2.2×10^6					
TS-5-2-1	.7	48.4	7.7			40.7	40.5	1.00
-2	1.7	48.4	7.7			40.7	40.0	1.02
-3	8.2	56.2	8.2			48.0	39.5	1.22
-4	8.7	56.2	8.3			47.9	39.3	1.22
-5	20.2	67.1	10.5			56.6	39.0	1.45
-6	29.4	79.6	12.8			66.8	39.0	1.71
-7	42.9	112.4	17.8		2.4	92.2	38.5	2.40
-8	47.9	131.1	20.8		6.6	104.0	38.5	2.70
-9	52.8	156.1	22.6		13.4	120.2	38.5	3.12

RUN NUMBER	VOID FRACTION	MEASURED PRESSURE	FRICTION LOSS	ACCEL LOSS	NON REC LOSS	CORR. PRES	SINGLE PHASE PRESS	PRES. RATIO
			P = 40 PSIG G = 2.7×10^6					
TS-5-3-1	23.5	9[illegible].6	15			78.6	55.8	1.41
-2	21.0	96.8	14.7			82.1	55.8	1.47
-3	48.8	196.6	28.7	5.9	11.3	150.7	55.8	2.70
-4	51.4	215.4	31	6.7	16.0	161.7	55.2	2.93
-5	54.2	237.2	33.5	10.0	20.3	173.4	55.0	3.15
-6	33.5	134.2	19.2	2.3		112.7	55.8	2.02
-7	35.8	138.9	20.2	1.8		116.9	55.8	2.09
			P = 60 PSIG G = 2.2×10^6					
TS-5-4-1	1.9	49.9	7.5			42.4	37.0	1.15
-2	9.9	56.2	8.9			48.2	36.8	1.31
-3	22.5	68.7	10.0			58.5	36.5	1.68
-4	24.2	71.8	10.3			61.5	36.5	1.68
-5	29.5	79.6	11.8			67.8	36.2	1.87
-6	45.5	118.6	17.0		4.1	97.5	36.0	2.71
-7	51.7	143.6	20.3		11.1	112.2	36.0	3.12
-8	53.0	149.8	21.0		12.9	115.9	35.8	3.24
-9	51.3	140.5	20.0		10.2	110.3	35.9	3.07
			P = 60 PSIG G = 2.7×10^6					
TS-5-3-1	30.6	118.6	16.5			102.1	53.5	1.91
-2	35.6	132.7	18.2			114.5	53.3	2.15
-3	42.6	163.9	21.5		3.6	138.8	53.1	2.61
-4	46.1	185.7	23.8	1.5	7.2	153.2	53.1	2.88

P = 60 PSIG G = 2.7×10^6

RUN NUMBER	VOID FRACTION	MEASURED PRESSURE	FRICTION LOSS	ACCEL LOSS	NON REC LOSS	CORR. PRESS	SINGLE PHASE PRESS	PRES. RATIO
TS-5-5-5	50.3	199.8	26.4	2.3	12.8	158.3	52.9	2.99
-6	52.7	224.7	28.5	2.0	18.4	175.8	52.5	3.35
-7	54.0	237.2	29.0	5.6	21.3	181.3	52.9	3.43

TS-6 σ = .247

P = 25 PSIG G = 2.1×10^6

TS-6-1-1	2.7	113.5	4.7			108.8	102.3	1.02
-2	3.5	113.5	4.7			108.8	"	1.02
-3	6.7	139.7	5.0			134.7	"	1.26
-4	13.8	165.9	5.7			160.2	"	1.50
-5	20.5	174.7	6.5			168.2	"	1.58
-6	29.6	209.6	8.0			201.6	"	1.89
-7	38.4	227.1	10.3	.3		216.5	"	2.03
-8	45.6	266.4	12.2	.7	11.4	242.1	"	2.37
-9	48.0	279.5	12.5	.8	16.0	250.2	"	2.45
-10	53.5	314.4	14.3	1.6	31.3	267.2	"	2.61
-11	56.9	366.8	16.2	2.2	45.3	303.1	"	2.96
-12	62.1	419.2	19.5	2.5	65.5	331.7	"	3.24
-13	65.2	471.6	21.8	2.4	85.0	362.4	"	3.54
-14	66.9	524.0	23.0	3.5	102.0	395.5	"	3.87
-15	68.3	559.0	25.5	3.3	111.3	418.9	"	4.09
-16	69.4	567.7	28.5	3.9	117.8	417.5	"	4.08

RUN NUMBER	VOID FRACTION	MEASURED PRESSURE
TS-6-2-1	28.6	192.2
-2	39.0	244.6
-3	45.2	266.4
-4	46.8	262.0
-5	50.2	297.0
-6	53.2	314.4
-7	58.4	358.1
-8	58.6	358.1
-9	61.7	384.3
-10	64.8	428.0
-11	65.3	436.7
-12	67.5	471.6
TS-6-3-1	2.2	179.1
-2	17.2	292.6
-3	19.5	305.7
-4	24.1	323.2
-5	24.6	327.5
-6	34.6	366.8
-7	33.4	366.8
-8	41.3	419.2

P = 40 PSIG G = 2.1×10^6

FRICTION LOSS	ACCEL LOSS	NON REC LOSS	CORR. PRESS	SINGLE PHASE PRESS	PRES. RATIO
4.2			188.0	102.3	1.84
5.4			239.2	"	2.34
6.3		10.4	249.7	"	2.44
6.6		14.0	241.4	"	2.36
7.0		21.8	268.3	"	2.62
7.9		30.7	275.9	"	2.70
9.5		48.8	299.8	"	2.93
9.5		48.8	299.8	"	2.93
10.5		61.7	312.1	"	3.05
12.0		79.0	337.0	"	3.29
12.5		80.6	343.6	"	3.36
13.5		93.9	364.2	"	3.56

P = 40 PSIG G = 2.9×10^6

4.7			174.4	174.4	1.00
5.7	.3		286.6	"	1.64
6.0	.3		299.4	"	1.72
6.6			316.6	"	1.82
6.7			320.8	"	1.84
8.6	.7		357.5	"	2.05
8.3	.7		357.8	"	2.05
10.3	.7	4.1	404.1	"	2.32

P = 60 PSIG G = 2.9×10^6

RUN NUMBER	VOID FRACTION	MEASURED PRESSURE	FRICTION LOSS	ACCEL LOSS	NON REC LOSS	CORR. PRESS	SINGLE PHASE PRESS	PRES. RATIO
TS-6-4-1	1.4	183.4	4.6			178.8	174.4	1.03
-2	11.6	257.7	5.2			252.5	"	1.45
-3	15.1	279.5	5.3			274.2	"	1.57
-4	28.2	331.9	6.8			325.1	"	1.86
-5	33.0	358.1	7.5			350.6	"	2.01
-6	37.5	384.3	8.2			376.1	"	2.16
-7	44.5	428.0	9.8		14.6	403.6	"	2.31
-8	50.1	471.6	11.6		34.5	425.5	"	2.44
-9	51.9	506.6	12.3		44.5	449.8	"	2.58
-10	50.1	480.4	11.6		35.2	433.6	"	2.49

P = 40 PSIG G = 4.6×10^6

(Avg. Void Fraction Used)

TS-6-5-1	1.3	406.1	10.0		.3	395.8	387.4	1.02
-2	8.1	506.6	10.5	2.8	1.8	491.5	387.4	1.27
-3	21.4	707.5	13.0	8.6	4.3	681.6	387.4	1.76
-4	32.8	812.3	15.8	16.6	6.2	773.7	387.4	2.00
-5	34.3	829.7	16.8	17.9	6.5	788.5	387.4	2.04
-6	18.9	672.5	12.5	7.5	3.8	648.7	387.0	1.67

	VOID FRACTION (%)			QUALITY (%)	
	INLET	AVG	OUTLET	INLET	OUTLET
TS-6-5-1	1.7	1.3	0.9	.04	.02
-2	4.8	8.1	11.4	.11	.28
-3	14.0	21.4	28.8	.35	.88
-4	22.6	32.8	43.0	.62	1.77
-5	23.8	34.3	44.9	.67	1.93
-6	12.1	18.9	25.7	.29	.74

Appendix D - Error Analysis

I. Error Computation

1. Instrument Accuracy

Differential Pressure Cell

Meter Face Output	±	3% full scale (2σ, from lit.)
Reading Error	±	.25% full scale (2σ, an est.)
Fluctuations	α < 25% ±	.25% full scale (2σ, an est.)
	α < 25% ±	1.0% full scale (2σ, an est.)

For test section #1, full scale = 60 in H_2O

For 60" H_2O in full scale = 312.12 PSF.

Meter Face Error = 9.36 PSF(2σ)

Reading Error = .78 PSF (2σ)

Fluctuation α < 25% = .78 PSF (2σ)

Then,

$$\alpha < 25\%;\ \sigma = \sqrt{(9.36/2)^2 + (.78/2)^2 + (.78/2)^2} = 4.712 \text{ or } 2\sigma = 9.42 \text{ PSF}$$

$$25\%;\ \sigma = \sqrt{(9.36/2)^2 + (.78/2)^2 + 3.12/2)^2} = 4.949 \text{ or } 2\sigma = 9.90 \text{ PSF}$$

Flow Meter

Orifice Calibration	±	1.0% of full scale for range used (est. of 2σ)
Meter Face Output	±	2.0% of full scale for range used (est. of 2σ)
Reading Error	±	.4% of full scale for range used (est. of 2σ)
Fluctuation	±	.4% of full scale for range used (est. of 2σ)

$$\sigma = \sqrt{.0100^2 + .002^2 + .002^2 + .0050^2} \quad \sigma = 1.15\% \text{ of full scale}$$

Void Sensor

Void Fraction Error (Calibration) $= \pm .05\ (2\sigma)$

Readout Error = 0 (digital voltmeter used)

Readout Fluctuation = $\pm$ .02

$$\sigma = \sqrt{(.025)^2 + (.01)^2} = .027\ (2.7\%)$$

Temperatures

a) Test Section

Thermometer Error $\pm$ 1% of full scale (from lit. $-\sigma$)

Reading Error 10°F (σ est.)

Fluctuations 0%

Since thermometer max. is 220°F, then 1% error = 2.2°F, so

$$\sigma = \sqrt{2.2^2 + 1^2} = 2.4°F$$

b) Fluid Temperature at Flow Meter

Thermometer Error $\pm$ 1% of full scale (est. = σ)

Reading Error $\pm$ 1°F (est. = σ)

Fluctuation Error 0%

Since thermometer max. is 300°F, then 1% = 3.0°F so

$$\sigma = \sqrt{3^2 + 1^2} = 3.2°F$$

Density error due to 3°F error ≈ 0.3% error in ρ.

System Pressure

Gage Error ± ½% f full scale (σ from lit.)

Reading Error ± ½psi (est σ)

Fluctuation ± ½ psi (est σ)

Since max gage reading is 150 psi, the ½% is .75 p. , so

$$\sigma = \sqrt{.75^2 + .5^2 + .5^2} = 1.0 \text{ psi } (\sigma)$$

2. Accuracy of Results including Propagation of Error

Flow

At 140°F (typical)ρ_g (for Freon 113) = 92.33 and at full scale, which is 100" H_2O, then

$$\text{Flow} = .080145 \sqrt{\rho_i \times 100" \ H_2O} = 7.70 \ lb_m/sec$$

(See Appendix B, "Calculation of Mass Flow")

For σ = 1.15% of full scale

σ = .089 lb/sec

at 5", flow = 1.72 lb_m/sec ± .089 σ = 5.2%

7½" fflow = 2.11 lb_m/sec ± .089 σ = 4.2%

10" flow = 2.44 lb_m/sec ± .089 σ = 3.6%

Note: Addition of the error in flow due to temperature measurement does not significantly change the above.

Pressure Ratio

In computing the error which may appear in the pressure ratio, consideration must be given not only to the pressure drop errors but those due to flow measurement. The pressure ratio is computed assuming a main flow rate which may be in error. The pressure ratio σ is then obtained by taking the square root of the sum of the squares of the pressure errors introduced by the flow and pressure drop measurement.

For example, at a flow indication of 5 inches of water and with 60" water full scale DP cell calibration, it is seen

at zero voids - Mean Press Ratio = 1.0 σ = .301

2σ error = 60%

at α = 30% Mean Press Ratio = 1.84 σ = .350

with 2σ error = 38%

at α = 60% Mean Press Ratio = 3.65 σ = .464

2σ error = 25.4%

Similiar calculations were performed for other flow rates and DP cell calibration ranges. The results are summarized in the section that follows.

II. Summary of Results - Pressure and Flow Errors

Test Section #1 Area Ratio = .590

TYPICAL ERRORS FOR VARIOUS CONDITIONS

Mass Flow Rate (G) lb_m/ft^2hr	Associated Errors: Flow Error (2σ) lb_m/hr	Pressure Ratio Error (2σ) α = 0%	α = 30%	α = 60%
$2.0x10^6$	± 10.4%	60%	38%	25%
$2.4x10^6$	± 8.4%	41%	26%	20%
$2.8x10^6$	± 7.2%	33%	21%	--

Test Section #2 Area Ratio = .595

TYPICAL ERRORS FOR VARIOUS CONDITIONS

Mass Flow Rate (G) lb_m/ft^2hr	Associated Errors: Flow Error (2σ) lb_m/hr	Pressure Ratio Error (2σ) α = 0%	α = 30%	α = 60%
$1.9x10^6$	± 10.4%	34%	27%	24%
$2.4x10^6$	± 8.4%	30%	25%	23%

Test Section #3 Area Ratio = .615

TYPICAL ERRORS FOR VARIOUS CONDITIONS

Mass Flow Rate (G) lb_m/ft^2hr	Associated Errors: Flow Error (2σ)	Pressure Ratio Error (2σ) α = 0%	α = 30%	α = 60%
$1.9x10^6$	± 10.4%	16%	12%	--
$2.3x10^6$	± 8.4%	14%	10%	--
$2.7x10^6$	± 7.2%	9%	8%	--

Test Section #4 Area Ratio = .505

TYPICAL ERRORS FOR VARIOUS CONDITIONS

Mass Flow Rate (G) lb_m/ft^2hr	Associated Errors: Flow Error (2σ) lb_m/hr	Pressure Ratio Error (2σ) α = 0%	α = 30%	α = 60%
$2.3x10^6$	10.4%	23%	22%	—
$2.8x10^6$	8.4%	19%	18%	—

Test Section #5 Area Ratio = .534

TYPICAL ERRORS FOR VARIOUS CONDITIONS

Mass Flow Rate (G) lb_m/ft^2hr	Associated Errors: Flow Error (2σ) lb_m/hr	Pressure Ratio Error (2σ) α = 0%	α = 30%	α = 60%
$2.2x10^6$	10.4%	30%	22%	—
$2.7x10^6$	8.4%	25%	20%	—

Test Section #6 Area Ratio = .249

TYPICAL ERRORS FOR VARIOUS CONDITIONS

Mass Flow Rate (G) lb_m/ft^2hr	Associated Errors: Flow Error (2σ) lb_m/hr	Pressure Ratio Error (2σ) α = 0%	α = 30%	α = 60%
$2.1x10^6$	3.6%	28%	16%	12%
$2.9x10^6$	2.6%	17%	11%	—

III. Error Analysis for Mixing Factors

For purposes of illustration, the data from test section 2 will be analyzed.

The errors are largest at the lower flows and vary with void fraction. For TS-2, the typical error in the original data will be

assumed to be at G = 1.9×10^6 and α = 30%. Under these conditions, the error in the data is 27%.

The data path line was fit graphically and may be considered analogous to taking a measurement of a value several times and then using an average. For such an averaging procedure, the improvement varies as $1/\sqrt{n}$. To determine the best line, 48 data points were used. Then

$$\text{error in line} = \text{data point error} \times 1/\sqrt{n}$$

$$= 27\% * 1/\sqrt{48} \simeq 3.9\% \ (2\sigma)$$

The above is the error in the location of the data path.

If the data path was exact (no error) there would still be another error in determining the mixing factor. The mixing was determined graphically, by observing where pressure ratios with known mixing factors intersected the data path. To obtain intermediate values for specific void fractions, an estimate was made. By inspection this error could result in a mixing factor error of $\pm$ .02 (2σ).

Now the effect of a 3.9% error in the elevation of the "best fit" line (determined earlier) must be estimated. The estimated errors are as follows:

if α = 20% estimated error $\simeq \pm$ .15 (2σ)

α = 40% estimated error $\simeq \pm$ .08 (2σ)

α = 50% estimated error $\simeq \pm$ .07 (2σ)

α = 60% estimated error $\simeq \pm$ .05 (2σ)

Then the total uncertainty at each void fraction would be

$$\alpha = 20\% \qquad \sigma = \sqrt{\left(\frac{.15}{2}\right)^2 + \left(\frac{.02}{2}\right)^2} = .0756$$

or $$2\sigma = .151$$

Similarly

$\alpha = 40\%$ $\sigma = .0412$ or $2\sigma = .087$

$\alpha = 50\%$ $\sigma = .0364$ or $2\sigma = .073$

$\alpha = 60\%$ $\sigma = .0269$ or $2\sigma = .054$

IV Summary of Results - Mixing Factors

Test Section #1

Typical Errors for Various Void Fractions

Void Fraction	Mixing Factor Error (2σ)
20	--
40	--
50	--
60	.05

Test Section #2

Void Fraction	Mixing Factor Error (2σ)
20	.15
40	.08
50	.07
60	.05

Test Section #3

Void Fraction	Mixing Factor Error (2σ)
20	.08
40	--
50	--
60	--

Test Section #4

Void Fraction	Mixing Factor Error (2σ)
20	.16
40	--
50	--
60	--

Test Section #5

Void Fraction	Mixing Factor Error (2σ)
20	--
40	--
50	.09
60	.06

Test Section #6

Void Fraction	Mixing Factor Error (2σ)
20	.12
30	.06
40	.05
50	.04
60	.01

Appendix E

Non-Recovery Correction Data

1. Data of Mendler[6]

The amount of recovery twelve inches from the point of expansion was determined from the graphs provided by the work of Mendler[6] on a steam-water system. These data were plotted in Figures E-1, E-2, & E-3 for the three area ratios (σ) investigated by Mendler[6]. From these graphs the following conclusions were drawn:

1. The degree of recovery is not very sensitive to the area ratio.
2. The recovery is nearly complete 12" from the expansion if the void fraction is less than 40%.
3. According to Mendler's[6] data on single phase expansion, the recovery inhibited under single phase conditions is faster than with a two phase fluid.
4. A pressure dependency is possible but not certain with the recovery.

The correction line in Figure 9 is shown in Figures E-1, E-2, and E-3. It is seen that the fit in E-3 is not as good as in E-1 and E-2. Since E-1 and E-2 more closely represented the geometry of equipment used in the Cincinnati investigation, these graphs were used to determine the correction for higher voids. Figure E-3 was used to locate the point where non-recovery first appears. A best fit line to the data in E-3 indicates non-recovery occurs in the region of 40% void fraction.

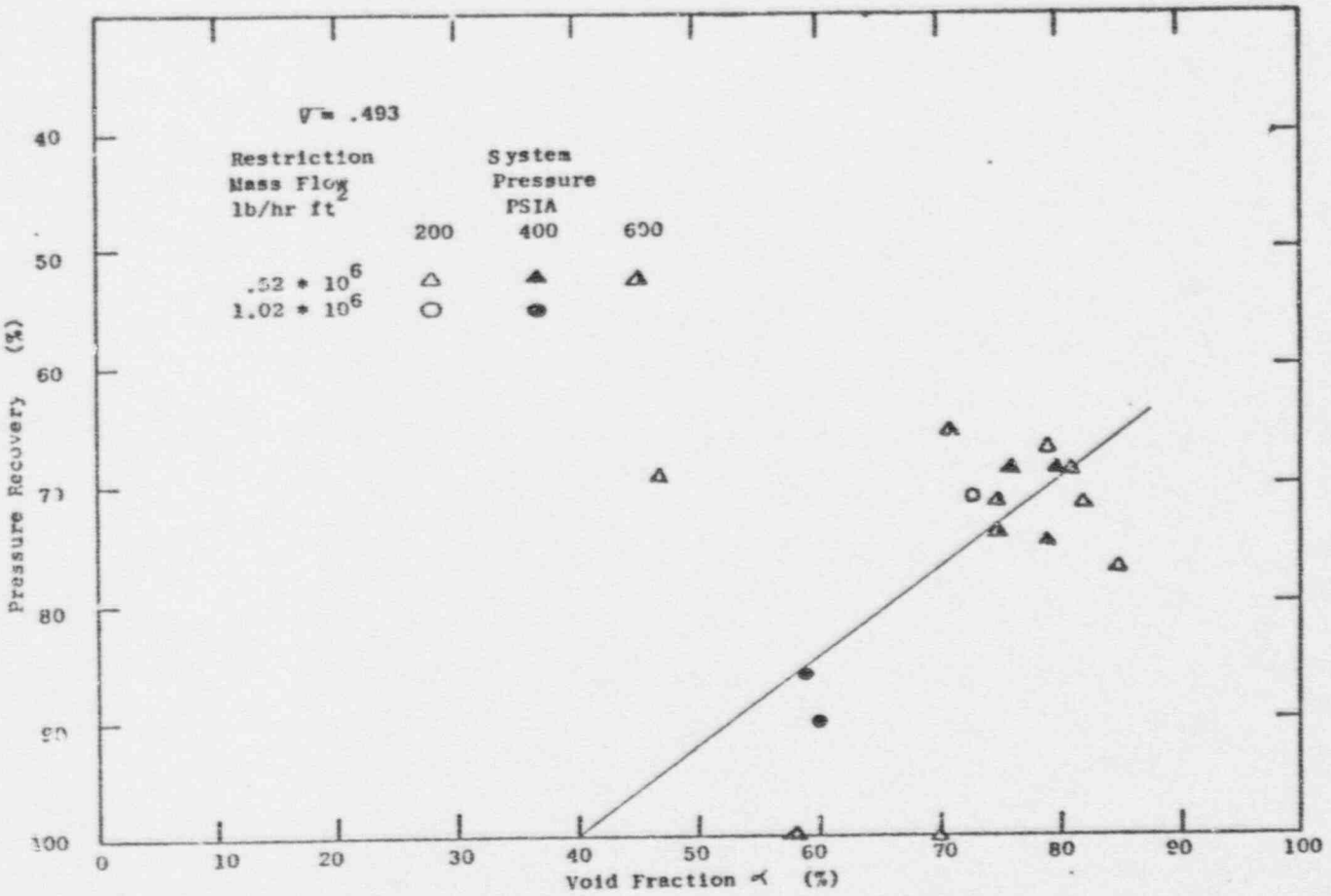

Figure E-1 Pressure Recovery vs Void Fraction 12 Inches From Expansion and $\bar{V}$ = .493

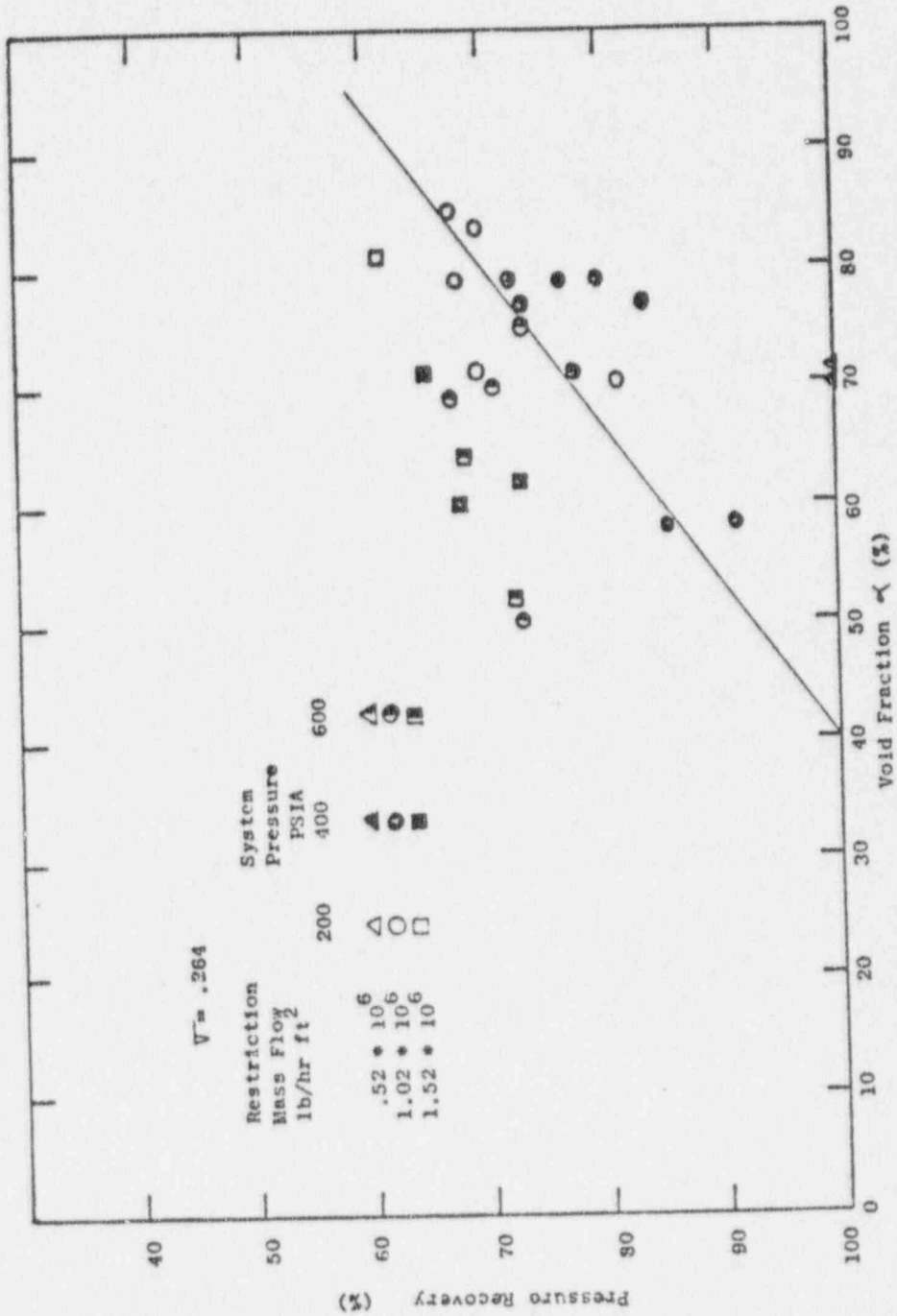

Figure E-2 Pressure Recovery vs Void Fraction 12 Inches From Expansion and V̄ = .264

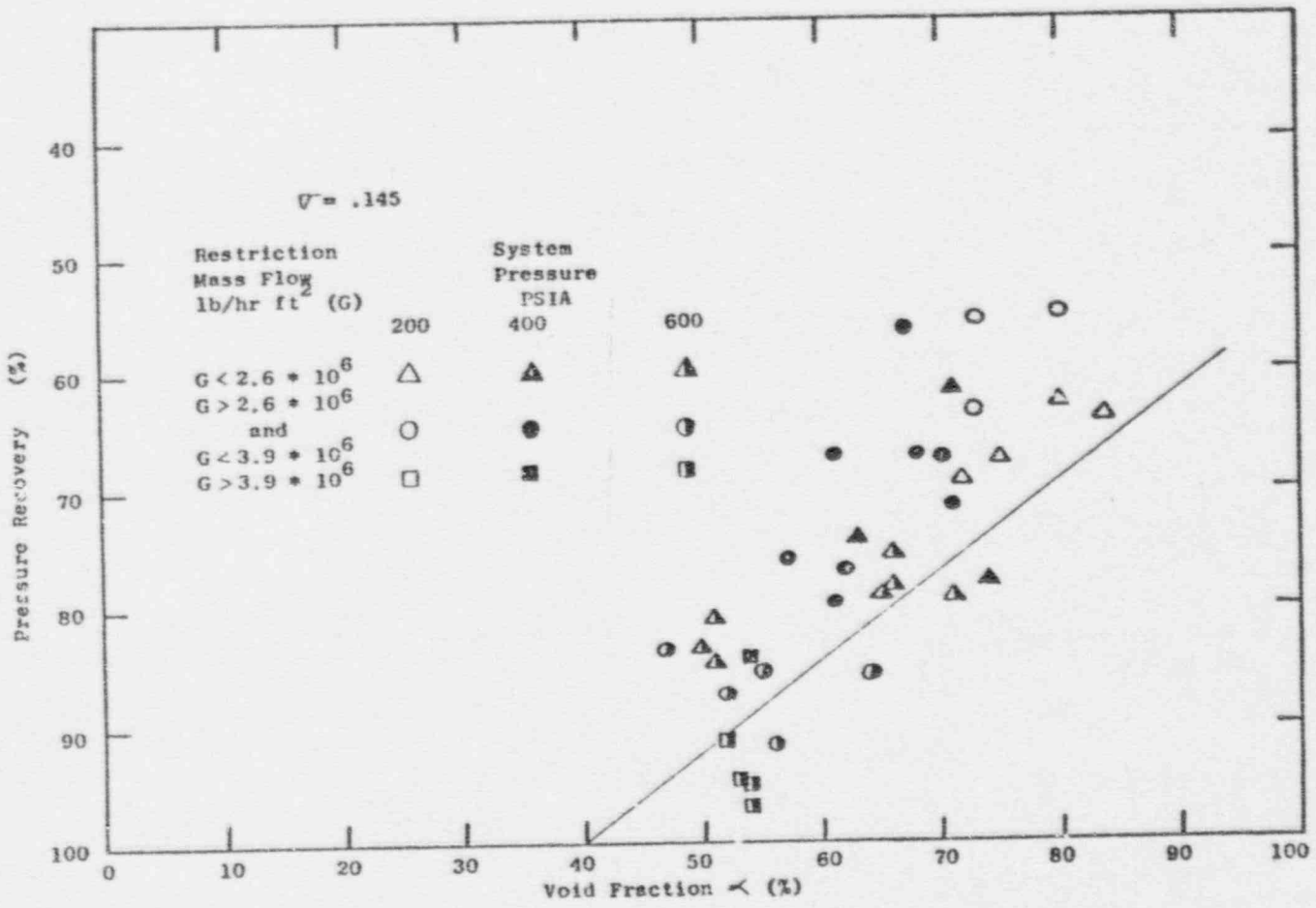

Figure E-3 Pressure Recovery vs Void Fraction 12 Inches From Expansion and $\bar{V}$ = . 145

2. Janssen and Kervinen[8] Non-Recovery Data

Janssen and Kervinen[8] investigated pressure recovery as a function of distance from the expansion for a short insert in a steam-water system. Figure F-1 shows the recovery for a single phase mixture and Figure F-2 shows that obtained with a two-phase mixture. The geometry used by Janssen is the same as that used by Cermak et al.[11].

From these graphs it is seen that the recovery is more rapid under single phase conditions than with a two phase mixture. The effects of non-recovery are more severe with single phase flow than with two phase flow if the pressure measurement is taken very close to the expansion.

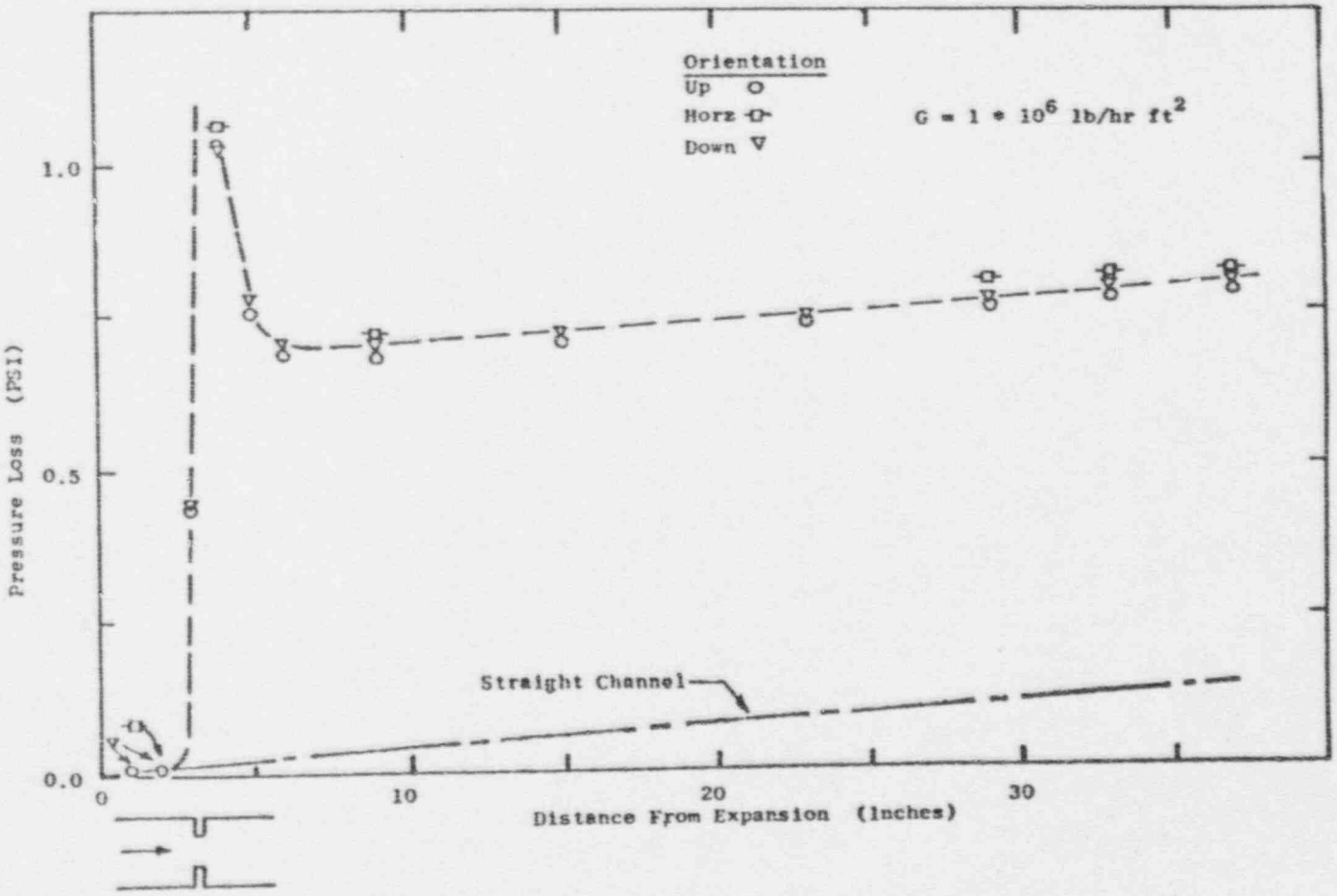

Figure F-1 Pressure Loss vs Distance From Expansion for Single Phase Flow

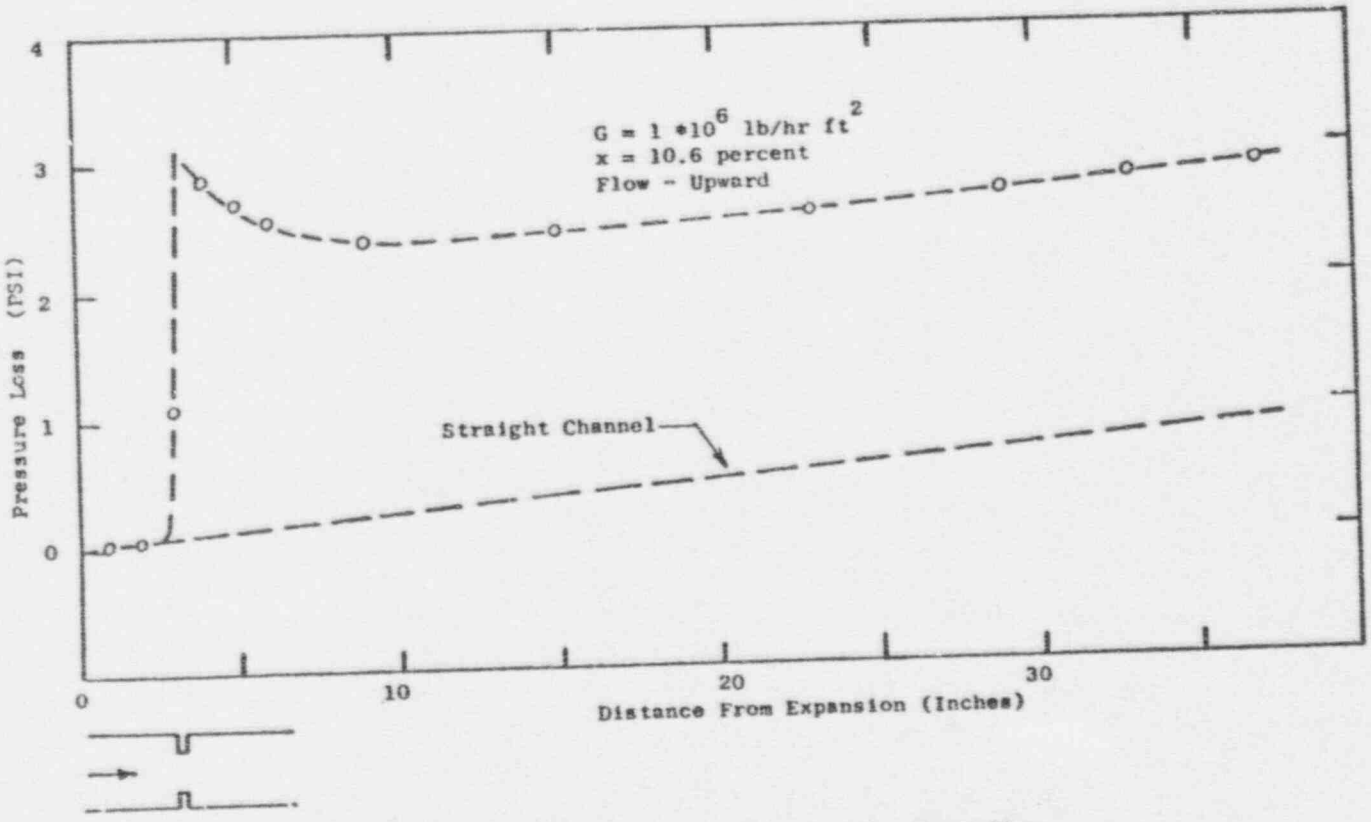

Figure F-2 Pressure Loss vs Distance From Expansion for Two-Phase Flow

Appendix F

Pressure Loss Calculation with Significant Vaporization Across the Restriction

The following data is from Run No. TS-6-5-5.

The freon properties were taken to be those at 180°F, the value of K was taken to be .723, the value of c to be .71, and σ = .249.

α_{inlet} = 23.8% $\quad x_{inlet}$ = .67% $\quad \rho_g$ = 1.211

α_{outlet} = 44.9% $\quad x_{outlet}$ = 1.93% $\quad \rho_\ell$ = 88.67

For the case where the quality (x, at the vena contracta is assumed to be the average of the inlet and outlet qualities, then

$$x_{vc} = \frac{x_{inlet} + x_{outlet}}{2} = \frac{.0067 + .0193}{2} = .013$$

$$\alpha_{slip_{vc}} = \frac{K}{[1 - \frac{\rho_g}{\rho_\ell}(1 - \frac{1}{x_{vc}})]} = .353$$

$$\alpha_{HOMOG} = \frac{x}{x+(1-x)(\sigma_g/\rho_\ell)} = .489$$

The average of the inlet and outlet void fraction is

$$\alpha_{avg} = \frac{\alpha_{inlet} + \alpha_{outlet}}{2} = \frac{.238 + .449}{2} = .344$$

or $\alpha_{avg} = 34.4\%$

From Figure 18, A = .54, then

$$\alpha_{vc} = \alpha_{SLIP} + A(\alpha_{HOMOG} - \alpha_{SLIP}) = .353 + .54(.489 - .353) = .426$$

By Substituting into Equation 12, we obtain

$$\Delta p_L \left(\frac{\text{SHORT}}{\text{INSERT}}\right) = \frac{[(4.6\times10^6)(.249)]^2}{(2)(4.17\times10^8)(.249)^2(88.67)} \frac{1}{(.71)^2}$$

$$\left[72.622\left(\frac{.013 + .0193}{2}\right)^2 \left(\frac{.426 + .449}{2}\right)\left(\frac{1}{(.426)^2} - \frac{(.249)^2(.71)^2}{(.449)^2}\right)\right.$$

$$+ \left(1 - \frac{.013 + .0193}{2}\right)^2 \left(1 - \frac{.426 + .449}{2}\right)\left(\frac{1}{(1 - .426)^2} - \frac{(.249)^2(.71)^2}{(1 - .449)^2}\right)$$

$$- 2(.249)(.71)\left\{72.622\left(\frac{.013 + .0193}{2}\right)^2 \left(\frac{1}{.426} - \frac{(.249)(.71)}{(.449)}\right)\right.$$

$$\left.\left. + \left(1 - \frac{.013 + .0193}{2}\right)^2 \left(\frac{1}{(1 - .426)} - \frac{(.249)(.71)}{(1 - .449)}\right)\right\}\right]$$

$$= 678.4 \text{ PSF}$$

END

DATE

FILMED

5-22-76

NTIS